

Borehole Environmental Tracers for Evaluating Net Infiltration and Recharge through Desert Bedrock

Victor M. Heilweil,* D. Kip Solomon, and Philip M. Gardner

ABSTRACT

Permeable bedrock aquifers in arid regions are being increasingly developed as water supplies, yet little is generally known about recharge processes and spatial and temporal variability. Environmental tracers from boreholes were used in this study to investigate net infiltration and recharge to the fractured Navajo Sandstone aquifer. Vadose zone tracer profiles at the Sand Hollow study site in southwestern Utah look similar to those of desert soils at other sites, indicating the predominance of matrix flow. However, recharge rates are generally higher in the Navajo Sandstone than in unconsolidated soils in similar climates because the sandstone matrix allows water movement but not root penetration. Water enters the vadose zone either as direct infiltration of precipitation through exposed sandstone and sandy soils or as focused infiltration of runoff. Net infiltration and recharge exhibit extreme spatial variability. High-recharge borehole sites generally have large amounts of vadose zone tritium, low chloride concentrations, and small vadose zone oxygen-18 evaporative shifts. Annual net-infiltration and recharge rates at different locations range from about 1 to 60 mm as determined using vadose zone tritium, 0 to 15 mm using vadose zone chloride, and 3 to 60 mm using groundwater chloride. Environmental tracers indicate a cyclical net-infiltration and recharge pattern, with higher rates earlier in the Holocene and lower rates during the late Holocene, and a return to higher rates during recent decades associated with anomalously high precipitation during the latter part of the 20th century. The slightly enriched stable isotopic composition of modern groundwater indicates this recent increase in precipitation may be caused by a stronger summer monsoon or winter southern Pacific El Niño storm track.

THE NAVAJO SANDSTONE forms an important part of the Dakota-Glen Canyon aquifer system in the Colorado Plateau region of the United States, which covers an area of about 210 000 km² in Utah, Arizona, Colorado, and New Mexico (Robson and Banta, 1995). It is a very uniform, well-sorted, fine- to medium-grained quartz eolian sand held together by calcite cement with prominent cross-bedding structures and secondary fracturing (Cordova, 1978). The Navajo Sandstone shares characteristics of both unconsolidated sediments and other consolidated rock formations. Because of its high primary permeability, movement of water through the sandstone matrix is more similar to flow through unconsolidated soils than through lower permeability bedrock. However, as in other exposed or shallowly buried bedrock formations, roots are present only in fractures. Conceptually, this limits transpiration losses and enhances

net infiltration and recharge compared with unconsolidated basin-fill sediments in similar arid settings. For this paper, the phrases “infiltration” and “net infiltration” are defined as vadose zone water movement below land surface and below the root zone, respectively. The maximum depth of the root zone is considered to be synonymous with the soil–bedrock contact because root penetration into the sparsely fractured sandstone is minimal. The phrase “Groundwater recharge,” or “recharge” for short, is defined as water entering the aquifer at the water table. It is assumed that all net infiltration eventually becomes groundwater recharge. Net-infiltration and recharge rates may be equivalent if conditions remain uniform while water is moving through the vadose zone to the water table.

Rapid population growth in the region and further development of groundwater resources requires quantification of groundwater recharge. Direct and focused net infiltration of precipitation on exposed outcrops or shallowly buried bedrock have been identified as the primary sources of recharge to the Navajo (Cordova et al., 1972, Cordova, 1978, 1981; Hood and Danielson, 1981; Eychaner, 1983; Hood and Patterson, 1984) and other fractured bedrock aquifers (Rasmussen and Evans, 1993; Flint et al., 2002). This is supported by vadose zone solute distributions observed along shallow trenches in the Navajo Sandstone of southwestern Utah (Heilweil and Solomon, 2004), indicating a connection between recharge and surficial characteristics such as soil coarseness and outcropping bedrock. Soil water sampling along these trenches showed that net infiltration readily penetrates sandstone beneath eolian sands as much as 3 m thick, whereas infiltration is unable to reach the soil–bedrock interface where finer-grained sandy loam and loamy sand deposits are thicker than 0.7 m.

The quantification of bedrock net infiltration and recharge is difficult, particularly in desert environments where infiltration is spatially and temporally variable. Regional watershed and groundwater-flow modeling often use empirical methods for estimating infiltration and runoff (Maxey and Eakin, 1950) that are not well suited for evaluating heterogeneity in recharge caused by localized climate, surface morphology, and geologic variables. Conversely, soil physics methods such as soil water and Darcy flux measurements (Nimmo et al., 1994) are limited by their time- and site-specific nature and may not accurately represent long-term recharge at the basin scale. Therefore, environmental-tracer methods were chosen for this study because of their ability to both

V.M. Heilweil and P.M. Gardner, U.S. Geological Survey, 2329 Orton Cir., Salt Lake City, UT 84119; D.K. Solomon, Univ. of Utah, 135 South 1460 East, Rm. 719 WBB, Salt Lake City, UT 84112. Received 10 Jan. 2005. *Corresponding author (heilweil@usgs.gov).

Published in Vadose Zone Journal 5:98–120 (2006).

Original Research

doi:10.2136/vzj2005.0002

© Soil Science Society of America

677 S. Segoe Rd., Madison, WI 53711 USA

Abbreviations: GNIP, Global Network of Isotopes In Precipitation; NWQL, National Water Quality Laboratory; TDTP, tritium depth-to-peak method; TMB, tritium mass-balance method; TU, tritium units; TU-m, tritium-unit meters.

integrate a range of temporal and spatial scales in the evaluation of recharge, as well as to quantify vadose zone travel times. As pointed out by others (Allison, 1988; Allison et al., 1994; Flint et al., 2002; Scanlon et al., 2002), the application of multiple tracer methods addresses this variability by providing flux estimates for these varying spatial and temporal scales. The objective of this study was to apply environmental tracer methods to estimate rates of net infiltration and recharge to the Navajo aquifer in Sand Hollow under current and past climates and to develop a general understanding of processes affecting recharge to exposed bedrock aquifers in arid regions.

SITE DESCRIPTION

The Sand Hollow study area is located in southwestern Utah along the western edge of the Navajo aquifer system of the Colorado Plateau (Fig. 1) (northernmost = 37.10°, southernmost = 37.00°, easternmost = 113.22°, westernmost = 113.25°). Altitudes within Sand Hollow range from about 900 to 1300 m. The area is considered arid, with a mean annual precipitation at nearby St. George, UT of 210 ± 70 mm (based on records for 1893 through 2003; Western Regional Climate Center, 2004). The Navajo Sandstone is as much as 350 m thick at Sand Hollow. The basin has fairly gentle topographic relief and the sandstone is either exposed at the surface or covered with a veneer of soil (<1.5 m). About 40% of the basin is covered by sand dunes and fine sands, mostly located in the southern (upland) area (Fig. 2). Finer-grained loams and loamy very fine sands cover about 50% of the basin. The Navajo Sandstone crops out in the remaining 10% of the basin. Caliche deposits are often present at the soil–bedrock contact, particularly beneath the loams and loamy sands. A main ephemeral wash drains the higher-altitude southern part of the basin. Even during the largest storms, however, surface water spreads out and infiltrates into the permeable soils at the northern end where the topographic slope decreases, rather than leaving the basin. A reservoir constructed during 2002 in the lower-altitude part of the basin is being conjunctively managed for both surface-water storage and groundwater recharge (Fig. 1 and 2). Monitoring-well construction for observation of vadose zone and groundwater response to this artificial recharge also provided an opportunity for evaluating net infiltration and recharge processes.

Because of low elevation and rainfall, the vegetation present at Sand Hollow includes shrubs, cacti, and grasses. The predominant shrubs include *Larrea tridentata* (Sessé & Moc. ex DC.) Coville (creosote/chapparal), *Artemisia filifolia* Torr. (sagebrush), *Coleogyne ramosissima* Torr. (blackbrush), *Ambrosia dumosa* (Gray) Payne (burrobrush/white bursage), *Gutierrezia sarothrae* (Pursh) Britt. & Rusby (rabbitweed/snakeweed), *Ephedra torreyana* S. Wats. (Mormon tea/Torrey joint-fir), *Atriplex confertifolia* (Torr. & Frém.) S. Wats. (shadscale saltbrush), and *Rhus trilobata* Nutt. (skunkbrush). The predominant cacti include *Opuntia* spp. (prickly pear, cholla) and *Yucca* spp. The 40% of the basin covered by sand has sagebrush, rabbitweed, blackbrush, Mormon Tea, yucca, and grasses. The 50% of the basin covered by finer-grained loams and

has creosote, blackbrush, burrobrush, rabbitweed, Mormon tea, prickly pear, cholla, and grasses. The 10% of the basin with outcropping sandstone has very sparse vegetation located only along fractures that allow root penetration. The deciduous shrubs (shadscale saltbrush and skunkbrush) are present in narrow zones directly beneath exposed sandstone that regularly receive runoff from the slickrock.

The underlying Navajo aquifer is unconfined, with depths to water in the central part of the basin ranging from 15 to 65 m below land surface. Vertical groundwater hydraulic gradients calculated from nested piezometers at Sites 13 through 17 and at Sites 42 and 43 are 0.006 and 0.003, respectively. Based on the distribution of potentiometric contours, these downward gradients of potentiometric contours, these downward gradients at Sand Hollow are consistent with a conceptual model in which net infiltration of precipitation through the vadose zone is the primary source of recharge to the aquifer (as opposed to other potential recharge sources, such as interbasin groundwater flow from higher-elevation areas).

THEORY

Chloride concentrations in atmospheric deposition and pore water (both within the vadose zone and beneath the water table) are often used for estimating rates of net infiltration and recharge. A simplified form of the Cl^- mass balance (CMB) method (Allison and Hughes, 1978; Allison, 1988; Dettinger, 1989; Wood and Sanford, 1995) can be represented as

$$q_{\text{CMB}} = \frac{[\text{Cl}]_{\text{dep}}}{[\text{Cl}]_{\text{pw}}} P \quad [1]$$

where q_{CMB} is the net-infiltration or recharge rate (L T^{-1}), $[\text{Cl}]_{\text{dep}}$ is the average Cl^- concentration of atmospheric deposition (M L^{-3}), $[\text{Cl}]_{\text{pw}}$ is the average Cl^- concentration of pore water (M L^{-3}), and P is the precipitation rate (L T^{-1}). Atmospheric Cl^- deposition includes Cl^- in both precipitation and dry dust accumulation. The CMB method is based on the assumptions that Cl^- deposition is constant with respect to time, that Cl^- is transported through the vadose zone to the water table in liquid phase and does not partition into solid or gas phases, and that Cl^- is geochemically conservative and has no sources or sinks within the porous media of the vadose zone or underlying aquifer (Scanlon, 2000). The simplified form of the CMB method represented by Eq. [1] additionally assumes that there is no surface water Cl^- run-on or run-off at each borehole site.

Chloride concentrations in atmospheric deposition, average annual precipitation, and the amount of vadose zone Cl^- accumulation are used to estimate the residence time, T_r , of vadose zone Cl^- :

$$T_r = \frac{M_{\text{Cl}}}{[\text{Cl}]_{\text{dep}} V_p} \quad [2]$$

where M_{Cl} is the total mass of Cl^- in a column of unit area containing vadose zone material between land surface and the water table (M) and V_p is the average annual volume of precipitation falling on a unit area of

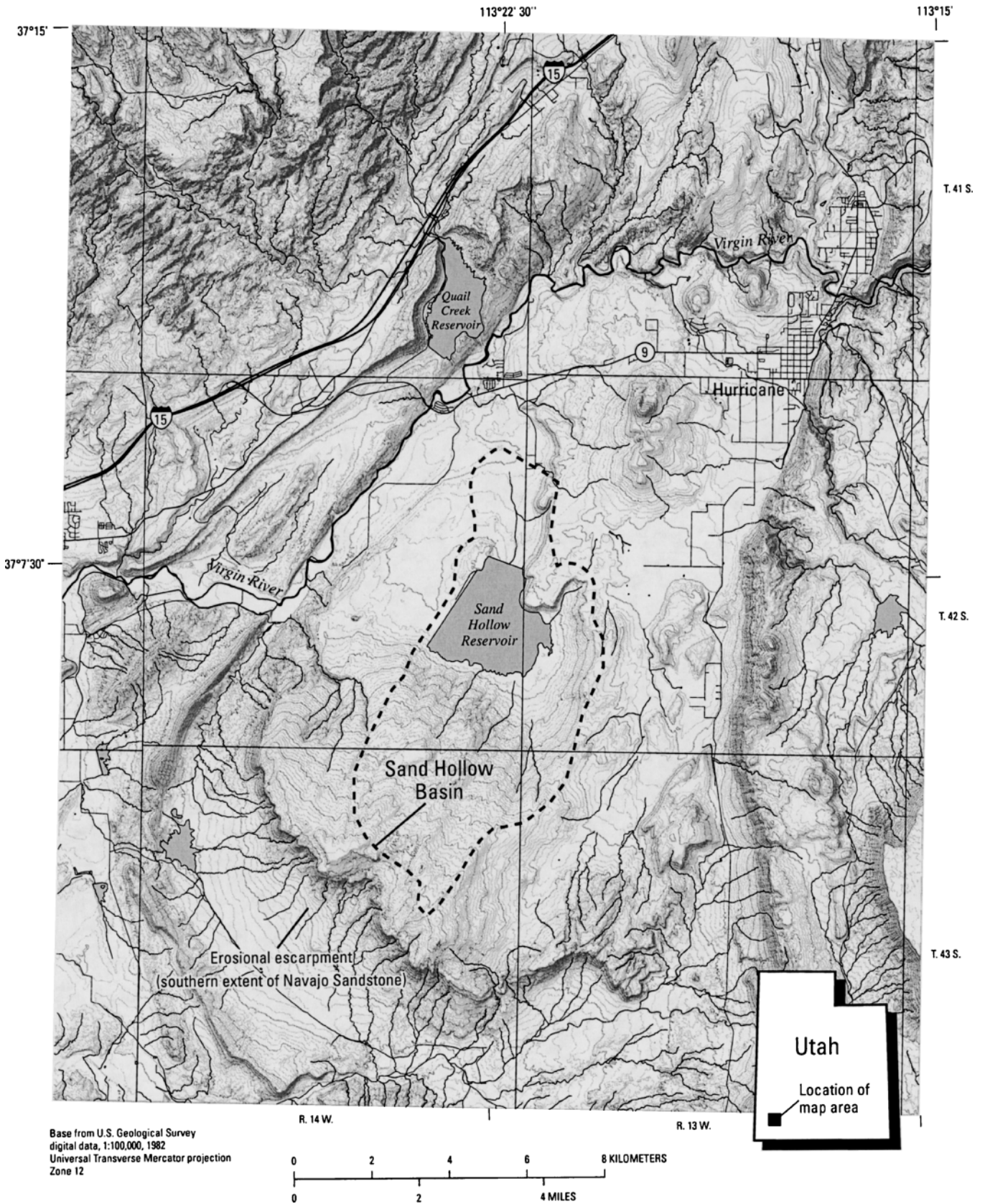
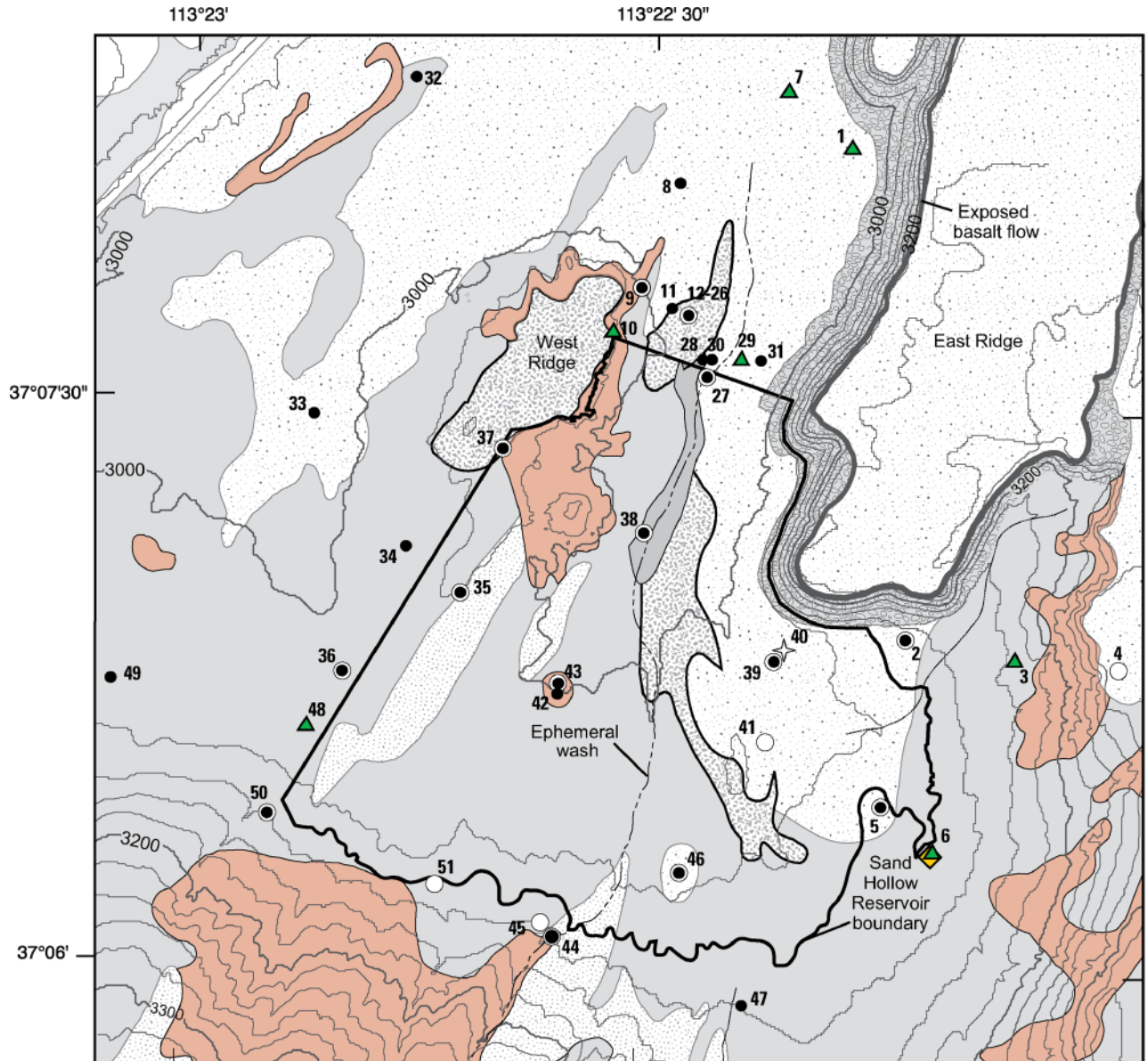
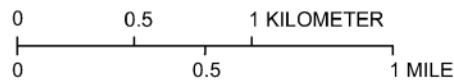


Fig. 1. Location of Sand Hollow, Washington County, Utah.



Base from U.S. Geological Survey digital data, 1:100,000, 1980
 Universal Transverse Mercator projection
 Zone 12



EXPLANATION

- | | | | |
|--|--------------------------|--|---|
| | Silty clay loam | | Sand Hollow Reservoir high-water boundary |
| | Fine sandy loam | | Ground-water monitoring well—Number refers to site number |
| | Loamy very fine sand | | Vadose-zone monitoring well |
| | Loamy fine sand | | Production well |
| | Fine sand dunes | | Vadose-zone borehole core-collection site |
| | Basalt boulder colluvium | | Meteorology station |
| | Exposed sandstone | | |

Fig. 2. Soils map with location of wells, borehole core-collection sites, and meteorology station in Sand Hollow, UT.

land ($L^3 T^{-1}$). M_{Cl} is calculated from a vertical profile of vadose zone pore-water concentrations and assumes that all the chloride is dissolved (in liquid state). Similar to the CMB method, the vadose zone Cl^- residence time calculation assumes that atmospheric Cl^- deposition is constant with respect to time and Cl^- behaves conservatively (geochemically) and has no sources or sinks within the vadose zone.

Vadose zone tritium concentrations are also used for evaluating net-infiltration rates (Allison and Hughes, 1978; Allison, 1988; Allison et al., 1994). Two commonly used methods are the tritium depth-to-peak (TDTP) method and the tritium mass balance (TMB) method. The TDTP method is based on depth below land surface of the 1963 3H precipitation peak. This peak from above-ground nuclear testing was originally more than two orders of magnitude above concentrations from natural 3H production. The net-infiltration rate, q_{TDTP} ($L T^{-1}$), can be estimated by the TDTP method using the equation (Cook et al., 1994)

$$q_{TDTP} = \frac{z}{t} \theta_v \quad [3]$$

where z is the vertical distance (L) between land surface and the 1963 3H peak, t is the length of time (T) between the 1963 3H peak and the sample collection time, and θ_v is the depth-weighted volumetric water content of the vadose zone between land surface and the 3H peak. The TDTP method assumes one-dimensional movement of water through the vadose zone and that volumetric water content throughout the profile does not change with time.

The tritium mass-balance (TMB) method, similar to the CMB method, is an application of the principle of continuity (conservation of mass). The method is based on the fraction of the mass of 3H measured in the vadose zone beneath the root zone compared with the decay-corrected mass of 3H estimated to have fallen as precipitation at the site. The difference between these two 3H masses is assumed to have been recycled back into the atmosphere through evapotranspiration. Because of the very small fractionation between tritiated water (3HHO) and normal water (H_2O), the loss of 3HHO directly mirrors the loss of normal H_2O to evapotranspiration. Multiplying the fraction of vadose zone 3H mass by the average annual precipitation provides the average annual net-infiltration rate. Therefore, higher net-infiltration rates result from larger ratios of the mass of 3H in the vadose zone compared with the mass of 3H in precipitation. The TMB equation (Cook et al., 1994) is defined as

$$q_{TMB} = \frac{\int_0^{\infty} \theta(z) [^3H(z)] dz}{\sum_{i=1}^{\infty} w_i [^3H_i] e^{-\lambda t}} \quad [4]$$

where q_{TMB} is the net-infiltration rate ($L T^{-1}$), $\theta(z)$ is the volumetric water content at depth z , $[^3H(z)]$ is the pore-water 3H concentration at depth z ($M L^{-3}$), w_i is a weighting function to correct for variations in annual net infiltration (the weighting function used for Sand Hollow was the ratio of precipitation during each year

(i) to mean annual precipitation), and λ (T^{-1}) is the decay constant for 3H [$\ln(2)/(12.32 \text{ yr})$], and $[^3H_i] e^{-\lambda t}$ is the decay-corrected 3H concentration in precipitation i years before present ($M L^{-3}$) where λ is the radioactive decay constant for tritium of 0.05576.

The use of the term *mass balance* for both the CMB and TMB methods requires further clarification. There is a fundamental difference between the CMB and TMB methods. In the CMB method, the Cl^- is conserved once it enters the subsurface and only water is lost through subsequent evaporation and transpiration. In contrast, 3H is not conserved in the vadose zone, but rather can be evaporated or transpired back into the atmosphere. Therefore, the TMB is a true mass balance, whereas the CMB would be more accurately described as a Cl^- enrichment method because it inherently assumes that all Cl^- is conserved within the subsurface.

The TMB method can also be presented in the simplified form

$$q_{TMB} = \frac{M_{VZ}}{M_{PPT}} P \quad [5]$$

where M_{VZ} is the total mass of tritium present in the vadose zone at the site in tritium-unit meters (M), M_{PPT} is the total mass of tritium estimated to have fallen as precipitation at the site in tritium-unit meters (M), and P is the average annual precipitation ($L T^{-1}$). M_{VZ} can be calculated by integrating the product of the measured water content (unitless fraction) and tritium concentration in tritium units (TU) ($M L^{-3}$) for each vertical sample interval by the interval length (L). M_{PPT} can be calculated by multiplying the decay-corrected average annual estimated atmospheric tritium concentration for the location by total annual precipitation for that year.

The TDTP method is considered more accurate than the TMB method primarily because it does not require knowledge of the 3H input function (the historical record of 3H in precipitation). The 3H input function is generally not known for each site and must be interpolated from sparsely located Global Network of Isotopes In Precipitation (GNIP) stations (International Atomic Energy Agency Global Network of Isotopes in Precipitation, 2004). For Sand Hollow, the nearest sites are Flagstaff, AZ, Salt Lake City, UT, and Albuquerque, NM, located at distances of 270, 425, and 650 km, respectively, each having different wind and climate patterns. Also, because no early 3H precipitation measurements were made at any of these stations, the Sand Hollow 3H input function before the early 1960s is based only on correlations with the Ottawa, Canada station located more than 3000 km to the northeast at a much more northerly latitude.

A high percentage of 3H within the shallow root zone may eventually be recycled into the atmosphere rather than becoming net infiltration, causing an overestimate of net-infiltration rates when 3H in the root zone is included in the total mass of vadose zone 3H . However, error associated with root zone 3H in the mass-balance calculation is not considered an important factor at the borehole sites in Sand Hollow because of the exposed or shallowly buried sandstone, where minimal root penetration occurs.

At borehole sites without the presence of a clearly discernible 1963 vadose zone ^3H peak, the TMB method must be used to estimate net infiltration. The three primary disadvantages of applying the TMB method at Sand Hollow are:

1. It will overpredict net infiltration at sites where surface-water run-on has occurred because this additional surface mass of ^3H would increase the denominator of Eq. [4] and [5], thus causing lower actual net infiltration.
2. The ^3H input function is not well constrained and must be interpolated from sparsely located GNIP stations.
3. The seasonal variation in ^3H concentrations in precipitation can affect the actual mass of ^3H being recharged, particularly at places such as Sand Hollow where net infiltration and recharge have large seasonal variations. In the spring, upward shifts of stability regions of the tropopause allow high ^3H concentrations to be mixed into the moist layer and precipitated (Eriksson, 1983), causing a summer maximum and corresponding winter minimum in precipitation ^3H concentrations.

The equations used for estimating uncertainty of atmospheric Cl^- deposition, net-infiltration, and recharge rates are provided in the Appendix.

MATERIALS AND METHODS

Environmental tracers used during this study include chloride (Cl^-), bromide (Br^-), tritium (^3H), deuterium (^2H), and oxygen-18 (^{18}O). These tracers were analyzed in atmospheric deposition (combined dry fall and wet fall), vadose zone pore water, and groundwater. Six-month composite atmospheric-deposition samples were collected with a 75-mm-diameter straight-sided Buchner funnel at a height of about 1 m above ground supported by a stake and connected with copper tubing to a 1-L plastic sample bottle buried about 0.3 m below ground (Friedman and others, 1992). A thin (10 mm) layer of mineral oil in the bottle was used to minimize evaporation of water. The range in Cl^- concentration from 6-mo atmospheric deposition samples was compared with Cl^- concentrations from individual storm events, which were collected with a 150-mm-diameter brass funnel draining into a 250-mL high-density polyethylene bottle (Heilweil, 2003). To sample both wet fall and dust deposition between storms, the funnels for both the individual storms and the multiple-month composite samples were not rinsed between sample collections.

Vadose zone core samples were collected at 18 sites in Sand Hollow to evaluate vadose zone solute accumulations (Fig. 2). Borehole core samples (63.5-mm diameter) from 13 of these sites were analyzed for chloride, stable isotopes, and/or tritium and are reported in this work (Fig. 3, Table 1). To minimize contamination of these pore waters with drilling fluids, cores were collected with a triple-tube continuous coring system with air. To minimize evaporative loss of water, the core samples were immediately heat-sealed in a layered aluminum/plastic laminate. Vadose zone matric potentials were measured with in situ head-dissipation probe measurements at four depths (4.6, 10.7, 18.3, 30.0 m) at Site 39. Groundwater samples were collected from turbine-shaft production wells, as well as in piezometers and boreholes with an air-driven submersible piston pump after purging a minimum of three casing volumes.

Chloride concentrations in precipitation were analyzed by ion chromatography at the U.S. Geological Survey in San Diego, California and at the U.S. Geological Survey National Water Quality Laboratory (NWQL) in Denver, Colorado, with detection limits 0.10 and 0.08 mg L^{-1} , respectively; Cl^- concentrations in pore-water leachates and groundwater were analyzed the U.S. Geological Survey NWQL, with a detection limit of 0.08 mg L^{-1} . Bromide concentrations in precipitation, pore-water leachates, and groundwater were analyzed by the Los Alamos National Laboratory in Los Alamos, NM, with a detection limit of 0.016 mg L^{-1} . Core samples for Cl^- and Br^- analysis were first weighed, then oven-dried at 105°C for 24 h to determine gravimetric water content. Based on replicate measurements, the uncertainty in gravimetric water content measurements is about 10% of the measured water content. Gravimetric water content was converted to volumetric water content assuming a bulk density of $1980 \pm 110 \text{ kg m}^{-3}$ ($n = 90$ samples). The dried sandstone samples were then mixed with an equal mass of deionized water to leach the salts. This leachate was centrifuged at 700 g for 2 h to remove silts and then filtered to 0.45 μm . Pore-water Cl^- and Br^- concentrations were then calculated from the leachate concentration and core sample water-content measurements.

Deuterium (^2H) and ^{18}O isotopic ratios of precipitation, vadose zone pore waters, and groundwater were analyzed with an isotope-ratio mass spectrometer at the University of Utah Stable Isotope Ratio Facility for Environmental Research. Tritium concentrations in precipitation, vadose zone pore water, and groundwater were analyzed at the University of Utah Dissolved Gas Service Center on a mass spectrometer by the helium in-growth method (Clark et al., 1976). Pore waters were extracted from core samples for isotopic analysis by cryodistillation. Pore-water tritium sample volumes were generally around 50 mL, and minimum in-growth holding times were about 12 wk. Uncertainty in the pore-water tritium analysis was generally <0.5 TU, with many samples being between 0.01 and 0.1 TU.

RESULTS

Chloride

The Cl^- concentration of atmospheric deposition is needed to calculate both vadose zone net-infiltration and groundwater recharge rates using the Cl^- mass-balance method. The precipitation-weighted mean concentration of atmospheric Cl^- deposition at the Sand Hollow weather station (elevation 940 m) is $0.8 \pm 0.3 \text{ mg L}^{-1}$, based on eight 6-mo atmospheric-deposition samples collected between June 1999 and September 2004, which ranged from 0.5 to 1.2 mg L^{-1} . The 0.3 mg L^{-1} standard deviation (1σ) results in an uncertainty in Cl^- deposition of about 38%. Three other 6-mo periods were excluded because of high sulfate concentrations, which indicate possible contamination from bird droppings, decaying insect debris, or dust associated with nearby construction (Table 2). The range in 6-mo composite Cl^- deposition values is similar to the range in Cl^- concentrations from individual storm events (Heilweil, 2003). The mean Cl^- concentration is larger than average annual Cl^- values between 1999 and 2003 at higher-elevation National Atmospheric Deposition Program sites in Bryce Canyon National Park (0.07–0.08 mg L^{-1} ; elevation 2480 m) and Grand Canyon National park (0.08–0.15 mg L^{-1} ; elevation 2150 m) (National Atmospheric Deposition

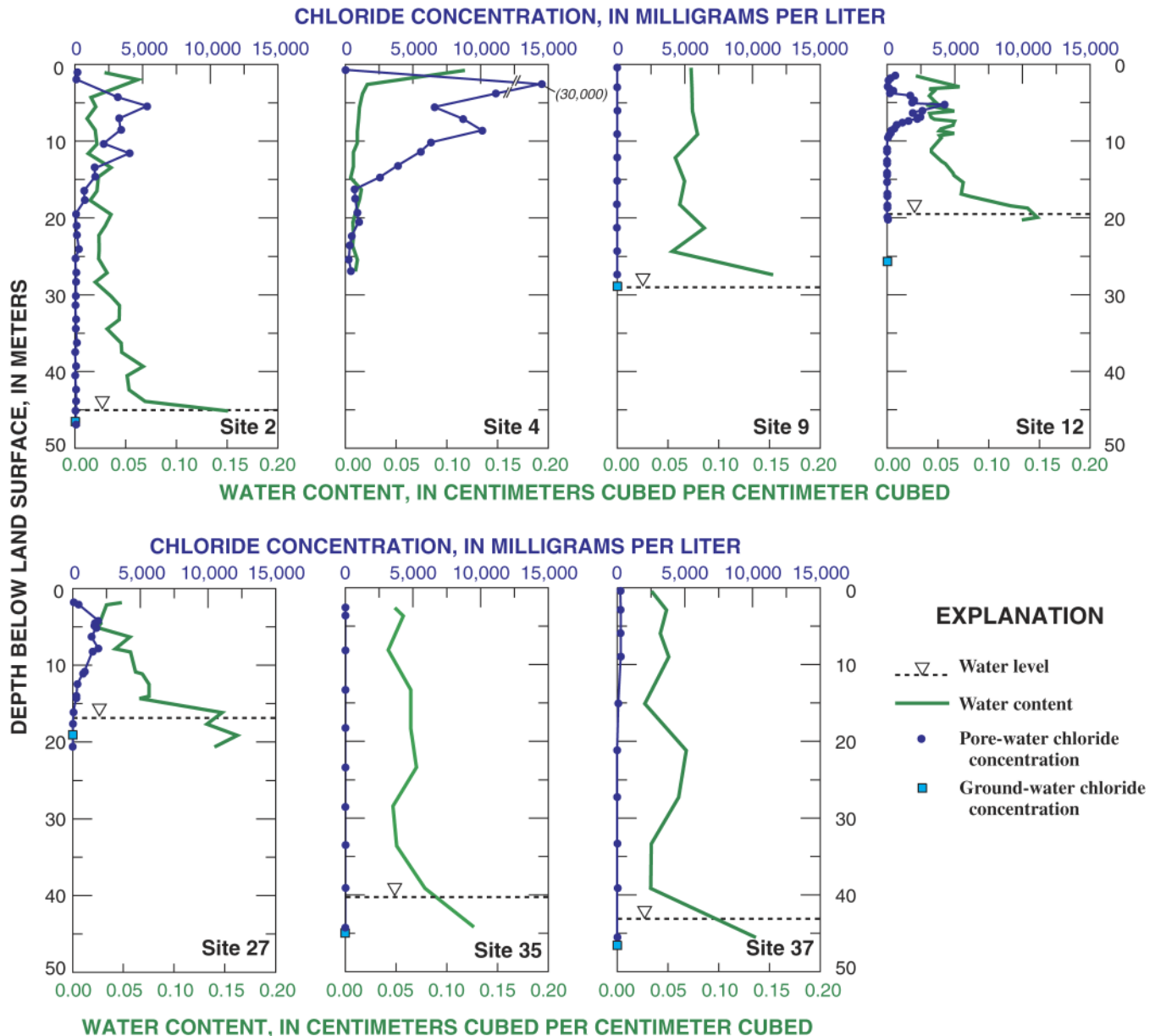


Fig. 3. Chloride concentration and volumetric water content of pore-water and groundwater samples collected at selected boreholes in Sand Hollow, UT.

Program, 1999–2003). However, the Cl^- concentrations at Sand Hollow are similar to those measured during the same period in Salt Lake City, Utah ($0.27\text{--}1.29\text{ mg L}^{-1}$; elevation 1300 m). Also, the bowl-shaped topography of Sand Hollow may be a natural dust trap, possibly causing an elevated dry-dust component of Cl^- deposition relative to regional values.

With an average estimated precipitation rate of $210 \pm 70\text{ mm yr}^{-1}$ at Sand Hollow, the precipitation-weighted mean Cl^- concentration of $0.8 \pm 0.3\text{ mg L}^{-1}$ was used to calculate a Cl^- deposition rate of $17 \pm 8.5\text{ }\mu\text{g } 100\text{ mm}^{-2}\text{ yr}^{-1}$. Leachates prepared from borehole-core samples show that accumulation of Cl^- in the vadose zone at Sand Hollow is quite variable. Total mass of Cl^- accumulation ranged from $4 \pm 0.7\text{ mg } 100\text{ mm}^{-2}$ (Sites 9 and 35) to at least $230 \pm 30\text{ mg } 100\text{ mm}^{-2}$ (Site 4) for a

vertical column of 10-mm horizontal length and 10-mm horizontal width by vertical depth (distance from land surface to the water table). As determined by Eq. [2] and [A5], the total masses of vadose zone Cl^- represent about 200 ± 100 to $12\,000 \pm 6\,000\text{ yr}$ of accumulation in Sand Hollow (Table 1). A cooler and wetter regional climate during the late Pleistocene (Weng and Jackson, 1999) likely precluded the accumulation of shallow vadose zone Cl^- before about 12 000 yr ago.

Vadose zone water content of the borehole-core samples is generally consistent with trends in vadose zone Cl^- accumulation. Mean vadose zone volumetric water content, calculated from land surface to the capillary fringe, ranged from 1.7 to 7.8% at the 13 borehole sites (Table 1, Fig. 3). Site 4 had the lowest average vadose zone water content (1.7%), consistent with the largest

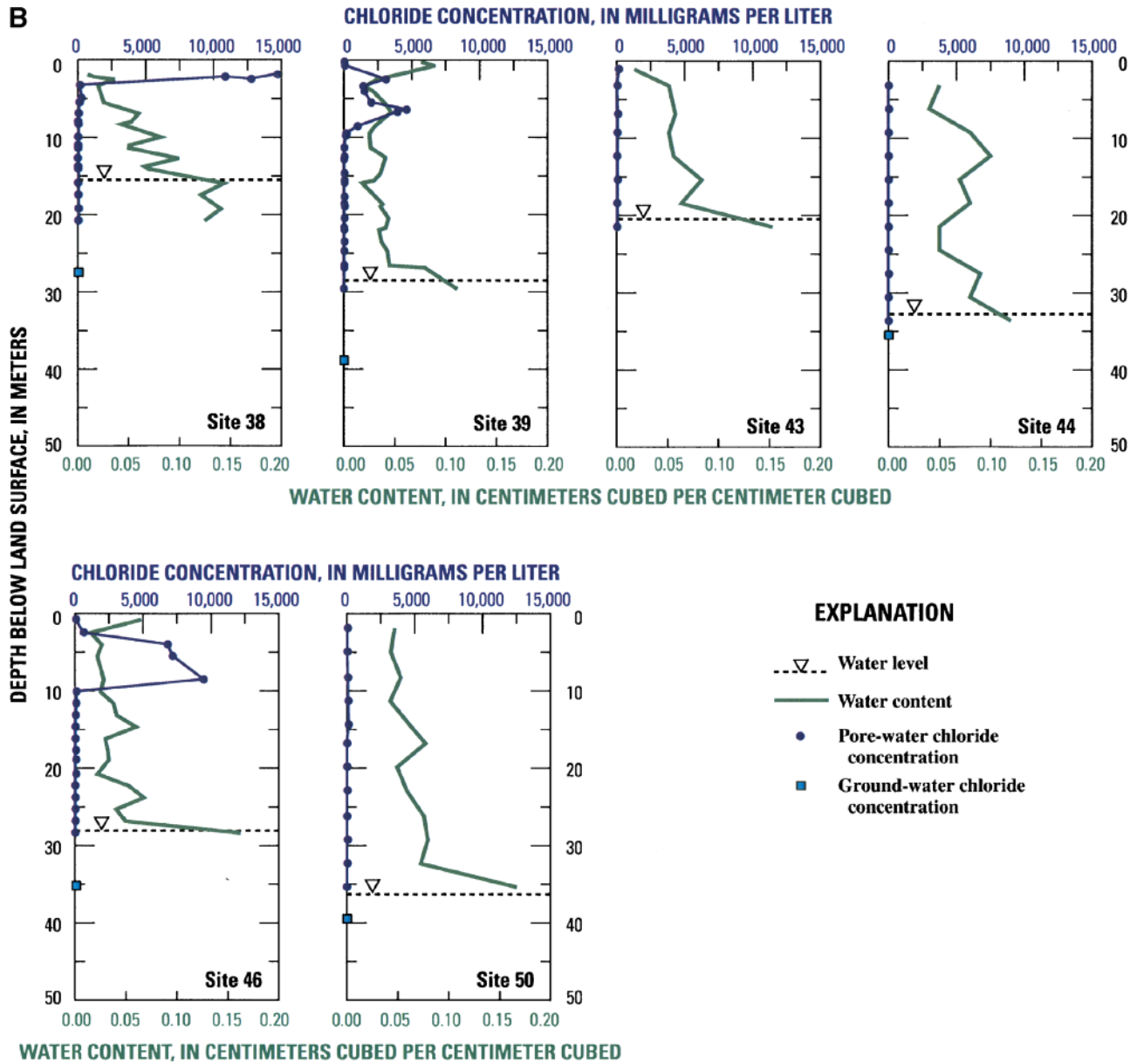


Fig. 3. Continued.

Cl⁻ accumulation of any of the sites within Sand Hollow. Site 4 is covered with finer-grained soils and is located on East Ridge (Fig. 2, Table 1), where more bare-soil evaporation likely occurs because of its increased exposure to wind. Site 9 had the highest average vadose zone water content (7.8%), consistent with having the smallest Cl⁻ accumulation. Located along a small side wash, this site regularly receives focused infiltration of surface-water runoff from the exposed sandstone of West Ridge.

The Cl⁻ profiles (Fig. 3) generally have the characteristic bulge shape observed in many desert soils (Phillips, 1994). The peak concentrations range from 28 mg L⁻¹ at Site 35 to 29 900 mg L⁻¹ at Site 4 (Table 1). Most of the profiles (Fig. 3) show shallow Cl⁻ accumulations within the sandstone beneath the root zone

and maximum concentrations occurring between 1.2 and 15 m below land surface (Table 1), with an average depth of about 5 m.

Net infiltration rates and uncertainties were calculated with the CMB method (Eq. [1], [A4]) using both (i) the average vadose zone Cl⁻ concentration of pore water from borehole samples between the soil-bedrock interface and the bottom of the Cl⁻ bulge and (ii) the average vadose zone Cl⁻ concentration below the Cl⁻ bulge. Because the Cl⁻ bulge at Sand Hollow is always in the sandstone and beneath the zone of root transpiration, calculations based on Cl⁻ concentrations within the bulge at Sand Hollow are considered to be net-infiltration rates. These rates likely represent net infiltration during the mid- to late Holocene and depend on the amount of Cl⁻ accumulation at each site. Based on pore-water Cl⁻ con-

Table 1. Vadose zone chloride parameters and water content from borehole-core samples, Sand Hollow, Utah. Refer to Fig. 2 for site locations.

Site	Site description	Depth to bedrock m	Total mass of vadose zone Cl ⁻ accumulation mg 100 mm ⁻²	Total duration of vadose zone Cl ⁻ accumulation [†] yr	Peak vadose zone Cl ⁻ concentration [‡] mg L ⁻¹	Depth of peak vadose zone Cl ⁻ concentration [§] m	Mean vadose zone volumetric water content [§] %	Duration of Cl ⁻ accumulation within bulge and percent of total accumulation yr, %	Mean vadose zone Cl ⁻ concentration from land surface to bottom of bulge mg L ⁻¹	Depth interval between Cl ⁻ bulge and water table [¶] m	Mean vadose zone Cl ⁻ concentration below bulge [#] mg L ⁻¹
9	fine sand/exposed sandstone beneath wash	0.0	4 ± 0.7	200 ± 100	41	8	7.8	100 (50%)	22 ± 4	9 to 28.8	13
35	sand dunes	0.4	4 ± 0.7	200 ± 100	28	5	5.9	50 (20%)	20 ± 3	8 to 24.4	21
44	fine sand/exposed sandstone	0.0	5 ± 0.8	300 ± 200	36	6	6.8	100 (30%)	21 ± 3	12 to 32.7	23
43	beneath wash	0.0	5 ± 0.7	300 ± 200	141	1	5.4	150 (50%)	76 ± 9	12 to 20.2	38
50	exposed sandstone	1.2	15 ± 2	800 ± 400	138	15	6.0	400 (50%)	100 ± 10	17 to 36.6	51
37	loamy very fine sand on ridge	0.2	22 ± 3	1000 ± 600	336	5	4.4	800 (70%)	240 ± 20	21 to 43.3	41
38	silty clay loam near wash	0.9	55 ± 6	3000 ± 1500	14 700	2	4.7	2500 (90%)	6500 ± 650	7 to 15.6	44
12	loamy very fine sand	0.8	56 ± 6	3000 ± 1500	4300	5	5.6	3000 (100%)	1100 ± 110	11 to 19.6	36
39	fine sandy loam	0.8	70 ± 8	4000 ± 2000	4600	7	4.0	3500 (90%)	1600 ± 160	11 to 28.2	48
27	fine sandy loam beneath wash	0.8	72 ± 8	4000 ± 2000	1900	8	4.6	3500 (90%)	1100 ± 110	16 to 17.7	59
2	fine sandy loam	1.5	91 ± 10	7000 ± 2500	5400	6	3.3	4000 (60%)	2200 ± 220	20 to 45.4	109
46	fine sandy loam	1.2	140 ± 20	7000 ± 3800	9500	9	3.8	7000 (100%)	3500 ± 350	13 to 28.3	58
4	fine sandy loam on ridge	1.5	230 ± 30 ^{††}	12 000 ± 6000 ^{††}	29 900	3	1.7	—	5600 ± 560	25 to 140 ^{‡‡}	354

[†] Assuming a 17 ± 8.5 μg 100 mm⁻² annual Cl⁻ atmospheric deposition rate.

[‡] Shown in Fig. 3.

[§] Calculated between land surface and the water table.

[#] Uncertainty in depth is estimated at 1.5 m, or one-half of the average vertical interval between sampling points.

[¶] For depths below the Cl⁻ bulge and above the water table, except for Site 4, which did not reach water table.

^{††} Minimum because borehole was not drilled to water table.

^{‡‡} Depth to water table extrapolated from nearby water levels.

centrations between land surface and the bottom of the Cl^- bulge, net-infiltration rates ranged from 0.03 ± 0.01 to $8 \pm 4 \text{ mm yr}^{-1}$; rates ranged from 0.5 ± 0.2 to $13 \pm 7 \text{ mm yr}^{-1}$ using pore-water Cl^- concentrations below the bottom of the Cl^- bulge (Table 3).

The borehole sites are divided into low versus high recharge on the basis of total vadose zone Cl^- accumulation, peak vadose zone Cl^- concentration, and net-infiltration rates. Sites 2, 4, 12, 27, 37, 38, 39, and 46 are considered low-recharge sites with $\geq 20 \text{ mg } 100 \text{ mm}^{-2}$ total Cl^- accumulation (Table 1), peak Cl^- concentrations $\geq 300 \text{ mg L}^{-1}$ (Table 1), and Cl^- -bulge net-infiltration rates $\leq 1 \text{ mm yr}^{-1}$ (Table 3). Sites 9, 35, 43, 44, and 50 are considered high-recharge sites, having $< 20 \text{ mg } 100 \text{ mm}^{-2}$ total Cl^- accumulation, peak Cl^- concentrations of $\leq 150 \text{ mg L}^{-1}$, and Cl^- -bulge net-infiltration rates $\geq 2 \text{ mm yr}^{-1}$. Based on the mass of Cl^- in these shallow bulges (depths varying from 7 to 25 m), the CMB rates represent net infiltration during recent centuries at the high-recharge sites and net infiltration back to about 7000 yr at the low-recharge sites (Table 1). Calculations done using vadose zone Cl^- concentrations from below the Cl^- bulge to the water table represent net infiltration during an earlier period of time, reaching back to about 12000 yr at low-recharge sites.

It is assumed that all of the pore-water and groundwater Cl^- at Sand Hollow is of atmospheric origin. The Navajo Sandstone is a clean, well-sorted, eolian sandstone containing no known evaporite or other salt deposits. However, because of the upward advective movement into the Navajo Sandstone of Cl^- -rich brines from underlying formations containing evaporite deposits, as documented at other study sites (Kimball, 1992; Naftz et al., 1997; Heilweil et al., 2000), Cl^-/Br^- ratios were examined to evaluate potential Cl^- contributions from geologic sources. Such geologic sources of Cl^- typically have Cl^-/Br^- ratios exceeding 1000, and the ratios increase with increasing Cl^- concentration (Davis et al., 1998). However, no such trend is evident in groundwater from Sand Hollow, and groundwater Cl^-/Br^- ratios are always < 500 (Fig. 4), with a mean and standard deviation of 230 ± 80 ($n = 31$). The mean and standard deviation of Cl^-/Br^- ratios for the atmospheric deposition samples is 125 ± 95 ($n = 8$; Table 2). This is consistent with the range of 100 to 200 reported by Davis et al. (2004) for the southwestern United States. Furthermore, vadose zone

pore-water Cl^-/Br^- ratios generally increase from land surface to the water table (Heilweil, 2003), consistent with a doubling in the mean Cl^-/Br^- ratio from 125 for atmospheric-deposition samples to 230 for groundwater samples. This indicates that some unsaturated zone process, such as preferential uptake of Br^- by plant roots, influences groundwater Cl^-/Br^- ratios rather than a geologic source of Cl^- .

Groundwater Cl^- concentration at 31 sites in Sand Hollow ranges from 2.9 to 61 mg L^{-1} , with a mean $[\text{Cl}_{\text{gw}}]$ of $22.5 \pm 12.5 \text{ mg L}^{-1}$. The values at each site are similar to vadose zone pore-water Cl^- concentrations determined from core samples at or near the water table (Fig. 3), validating the leachate process for determining Cl^- concentrations from pore waters in cores. The wide range of Cl^- concentration in groundwater indicates that the amount of evaporative concentration of infiltrating precipitation in the shallow root zone is either spatially or temporally variable. Assuming a mean atmospheric deposition Cl^- concentration $[\text{Cl}_{\text{dep}}]$ of $0.8 \pm 0.3 \text{ mg L}^{-1}$ and a mean annual precipitation (P) at Sand Hollow of $210 \pm 70 \text{ mm}$, applying the CMB method (Eq. [1], [A4]) to these individual groundwater sites results in recharge rates ranging from 3 ± 1.4 to $60 \pm 29 \text{ mm yr}^{-1}$ (Table 3).

Tritium

The estimated ^3H concentration of precipitation at Sand Hollow from 1950 to 2000 is shown in Fig. 5, based on a distance-weighted average from monitoring stations at Albuquerque, NM; Flagstaff, AZ; and Salt Lake City, UT. The maximum ^3H concentration of precipitation during the aboveground nuclear testing in 1963 was estimated to exceed 2000 TU. Present ^3H concentrations in precipitation at Sand Hollow are near or slightly above the pre-bomb background levels. Three samples of recent precipitation (1999–2001) had measured ^3H concentrations ranging from 9.1 to 21.0 TU (Table 2). A surface-water sample collected during an ephemeral flow event on 9 Nov. 2002 had a ^3H concentration of only 2.3 TU, possibly caused by a dilution with older (lower ^3H) shallow vadose zone pore waters flushed into the wash by the infiltrating precipitation.

Vadose zone pore waters from boreholes within Sand Hollow had ^3H concentrations ranging from 0 to 17.9 TU (Fig. 6). Tritium concentrations of 4 to 12 TU were generally measured within the first few meters of land surface and likely represent recent precipitation. Profiles at Sites 35, 37, 39, 43, 44, and 50 show vadose zone peaks consistent with the peak atmospheric ^3H concentrations of the early 1960s. Profiles at Sites 2, 12, 27, and 38 do not display a prominent subsurface ^3H peak. Tritium concentrations at Site 9 were about 4 TU or greater throughout the entire vadose zone, indicating that the 1963 peak has already been flushed down to the water table. At each site, groundwater ^3H concentrations are generally similar to concentrations in pore waters from borehole cores at or near the water table. This gives confidence in cryodistillation methods used for pore-water ^3H extraction, particularly for core samples with higher water contents.

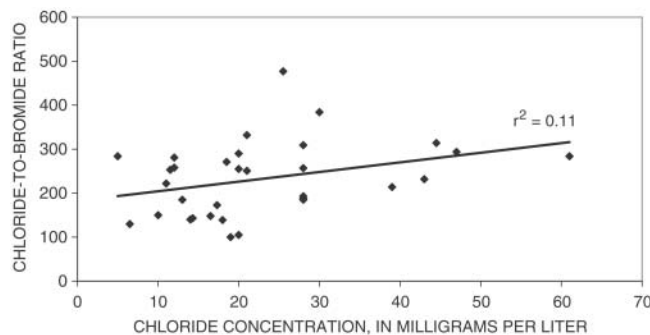


Fig. 4. Relation of chloride/bromide ratio to chloride concentration in water from selected wells in Sand Hollow, UT.

Table 2. Selected chemical constituents measured in precipitation samples collected in Sand Hollow, UT. Refer to Fig. 2 for site number. Anions were analyzed by USGS, San Diego, CA, unless noted.

Site	Sample date	Anions			Cl ⁻ /Br ⁻ ratio	δ ² H	δ ¹⁸ O	³ H
		Cl ⁻	Br ⁻ †	SO ₄				
		mg L ⁻¹			‰		TU	
2	30 Apr. 1999	—	—	4.7§	—	—	21 ± 1	
6	3 June 1999–12 Oct. 1999‡	6§	—	—	—	-76.0	-7.5	
6	12 Oct. 1999–13 Apr. 2000‡	1.2	0.007¶	3.0	171	-82.0	-11.0	
6	13 Apr. 2000–11 Oct. 2000‡	0.9	0.016	4.0	56	-21.0	-4.3	
6	11 Oct. 2000–30 Apr. 2001‡	1.2	<0.016	4.0	—	-86.0	-11.8	
6	30 Apr. 2001–3 Oct. 2001‡	3.5§	—	14§	—	-1.0	2.8	
6	3 Oct. 2001–8 May 2002‡	0.9	—	3.0	—	—	—	
6	8 May 2002–11 Sept. 2002‡	1.0	—	4.0	—	—	—	
6	11 Sept. 2002–8 May 2003‡	0.5	0.05	<3.0	—	-97.6	-13.0	
6	8 May 2003–8 Oct. 2003‡	0.5	<0.3	3.0	—	—	—	
6	8 Oct. 2003–4 May 2004‡	0.4	<0.3	2.3	—	—	—	
6	4 May 2004–22 Sept. 2004‡	1.6§	<0.3§	11§	—	—	—	
12	10 Oct. 2000	—	—	—	—	-43.0	-7.1	
12	11 Oct. 2000	1.7	0.007¶	2.6	243	-16.9	-2.6	
12	23 Oct. 2000	7.2§	1.129§	10.8§	—	-122.1	-13.8	
12	27 Oct. 2000	—	—	—	—	-72.1	-11.1	
12	28 Oct. 2000	—	—	—	—	-116.9	-15.3	
12	1 Nov. 2000	—	—	—	—	-79.2	-10.7	
12	10 Nov. 2000	0.8	0.023	1.6	37	-52.3	-9.2	
12	13 Nov. 2000	—	—	—	—	-49.1	-8.8	
12	12 Dec. 2000	—	—	—	—	-84.6	-10.5	
12	9 Jan. 2001	0.8	—	3.9	—	-84.6	-10.8	
12	12 Jan. 2001	0.3	<0.016	0.7	—	-91.0	-11.6	
12	14 Feb. 2001	—	—	—	—	-87.0	-12.7	
12	27 Feb. 2001	—	—	—	—	-126.4	-15.5	
12	1 Mar. 2001	0.3	<0.016	0.7	—	-104.1	-14.2	
12	5 Mar. 2001	0.4	<0.016	1.3	—	-112.1	-15.1	
12	7 Mar. 2001	0.4	<0.016	1.6	—	-104.5	-12.0	
12	9 Mar. 2001	—	—	—	—	-100.6	-13.7	
12	12 Mar. 2001	0.4	<0.016	1.3	—	-100.6	-13.7	
12	6 Apr. 2001	2.2§	<0.016§	11.2§	—	-34.2	-6.2	
12	9 Apr. 2001	—	—	—	—	-51.6	-7.2	
12	14 May 2001	16.6§	0.615§	29.9§	—	4.2	0.5	
12	17 May 2001	0.5	0.007¶	1.5	71	—	—	
12	28 May 2001	1.8§	0.0198§	4.71§	—	—	—	
12	26 June 2001	2.1§	0.0277§	8.41§	—	—	—	
12	5 July 2001	0.6	0.007¶	2.2	84	—	—	
12	9 July 2001	2.9	0.010¶	3.0	287	—	—	
12	11 July 2001	16.7§	0.620§	28.4§	—	—	—	
12	7 Oct. 2001	4.3§	0.190§	25.1§	—	-54.3	-6.7	
12	13 Nov. 2001	—	—	—	—	-39.0	-5.6	
12	25 Nov. 2001	—	—	—	—	-73.0	-9.2	
12	30 Nov. 2001	—	—	—	—	-103.0	-14.6	
12	4 Dec. 2001	—	—	—	—	-59.0	-8.5	
12	15 Dec. 2001	—	—	—	—	-84.0	-11.5	
12	23 Dec. 2001	—	—	—	—	-103.0	-13.3	
42	11 Sept. 2001	—	—	—	—	-3.1	3.3	
44#	9 Nov. 2002	0.32	0.006	2.3††	53	-48.2	-6.6	

† Analyzed by Los Alamos National Laboratory in Los Alamos, NM.

‡ Multiple-month atmospheric deposition sample collected at meteorology station.

§ Value is suspect; high sulfate (>4.0 mg L⁻¹) or phosphate concentration indicates contamination.

¶ Reported bromide concentration is less than the 0.016 ppm detection limit because of evaporative concentration.

Ephemeral flow event.

†† Analyzed by the USGS National Water-Quality Laboratory in Denver, CO.

Net-infiltration rates and uncertainties were calculated with the TDTP method (Eq. [3] and [A6]) at seven borehole sites, with rates ranging from 2.6 ± 1.2 to more than 57 ± 7 mm yr⁻¹ (Table 4). The uncertainties were calculated by using a standard deviation of 1.5 m for depth of the ³H peak (one-half the 3.0-m vertical interval between sample points), a standard deviation for water content of 10% of the measured values, and a standard deviation of 1 yr for the time since the atmospheric ³H peak. The highest net-infiltration rates are located at Sites 9 and 44, having a thin layer of fine sand overlying sandstone along ephemeral washes or rivulets that receive surface-water runoff from nearby exposed sandstone during storms ($\geq 57 \pm 7$ and 34 ± 5 mm yr⁻¹, respectively). Because the

1963 ³H peak has already been flushed out of the 29-m-thick vadose zone at Site 9, the actual net infiltration rate may be >57 mm yr⁻¹. Medium net-infiltration rates were measured along nearly flat-lying exposed sandstone at Site 43 and beneath nonvegetated sand dunes at Site 35 (26 ± 3 and 27 ± 4 mm yr⁻¹, respectively). This is consistent with a Navajo Sandstone infiltration study in the Dirty Devil River basin of south-central Utah, where measured infiltration rates were higher at locations covered with thin deposits of unconsolidated soils than beneath exposed sloping sandstone (Danielson and Hood, 1984). It is assumed that steeply dipping areas of exposed sandstone away from ephemeral wash channels in Sand Hollow would have net-infiltration rates less than about

Table 3. Summary of environmental-tracer data and recharge rates for borehole sites, Sand Hollow, UT. Refer to Fig. 2 for site numbers.

Site	Environmental-tracer data					Net infiltration and recharge rates				
	Total duration of vadose zone Cl ⁻ accumulation yr	Groundwater Cl ⁻ concentration mg L ⁻¹	Groundwater ³ H concentration [†] TU	Avg. vadose zone ¹⁸ O shift ‰	Groundwater deuterium ratio ‰	Vadose zone Cl ⁻ from soil-bedrock interface to bottom of bulge	Vadose-zone Cl ⁻ from bottom of bulge to water table mm yr ⁻¹	Groundwater Cl ⁻	Vadose-zone ³ H	
9	200 ± 100	2.9	6.9 ± 0.3	2.1	-79	8 ± 4	13 ± 7	60 ± 29	>57 ± 7	
35	200 ± 100	6.5	4.3 ± 0.2	-	-82	8 ± 4	8 ± 4	26 ± 13	26 ± 3	
44	300 ± 200	10.0 [‡]	4.1 ± 0.4	2.3	-83 [‡]	8 ± 4	7 ± 4	17 ± 8	34 ± 5	
43	300 ± 200	16.5 [‡]	1.0 ± 0.07	2.8	-84 [‡]	2 ± 1	4 ± 2	10 ± 5	27 ± 4	
50	800 ± 400	18.0	0.21 ± 0.09	3.4	-85	2 ± 1	3 ± 2	9 ± 4	10 ± 2	
37	1000 ± 600	20.4 [‡]	0.00 ± 0.01	3.0	-88 [‡]	0.7 ± .4	4 ± 2	8 ± 4	4.6 ± 2.1	
38	3000 ± 1500	61.1 [‡]	0.07 ± 0.21	2.2	-86 [‡]	0.03 ± .01	4 ± 2	3 ± 1.4	2.4 ± 1.2 [§]	
12	3000 ± 1500	19.9	0.00 ± 0.01	3.5	-84 [‡]	0.2 ± .1	5 ± 2	8 ± 4	2.8 ± 1.2 [§]	
39	4000 ± 2000	11.3 [‡]	0.07 ± 0.06	3.5	-85 [‡]	0.1 ± .05	4 ± 2	15 ± 7	2.6 ± 1.2	
27	4000 ± 2000	28.1	0.27 ± 0.10	4.1	-86 [‡]	0.2 ± .1	3 ± 1	6 ± 3	4.0 ± 1.8 [§]	
2	7000 ± 2500	21.0 [‡]	0.02 ± 0.06	3.8	-85 [‡]	0.08 ± .04	2 ± 1	8 ± 4	4.2 ± 2.2 [§]	
46	7000 ± 3800	10.9 [‡]	0.18 ± 0.06	3.7	-87 [‡]	0.05 ± .02	3 ± 1	15 ± 7	-	
4#	12 000 ± 6000	-	-	4.7	-	0.03 ± .01	0.5 ± .2	-	-	
Mean	1700 ^{††}	15 ^{††}	1.4 [‡]	3.3 [‡]	-85 [‡]	0.4 ^{††}	4 ^{††}	11 ^{††}	9 ^{††}	

[†] Analysis with highest precision listed when multiple values were available.

[‡] Arithmetic mean of multiple values.

[§] Calculated using ³H-mass-balance method multiplied by a correction factor of 2.

^{||} From shallowest port (1.4 m below water table).

[#] Borehole was not drilled to water table.

^{††} Geometric mean.

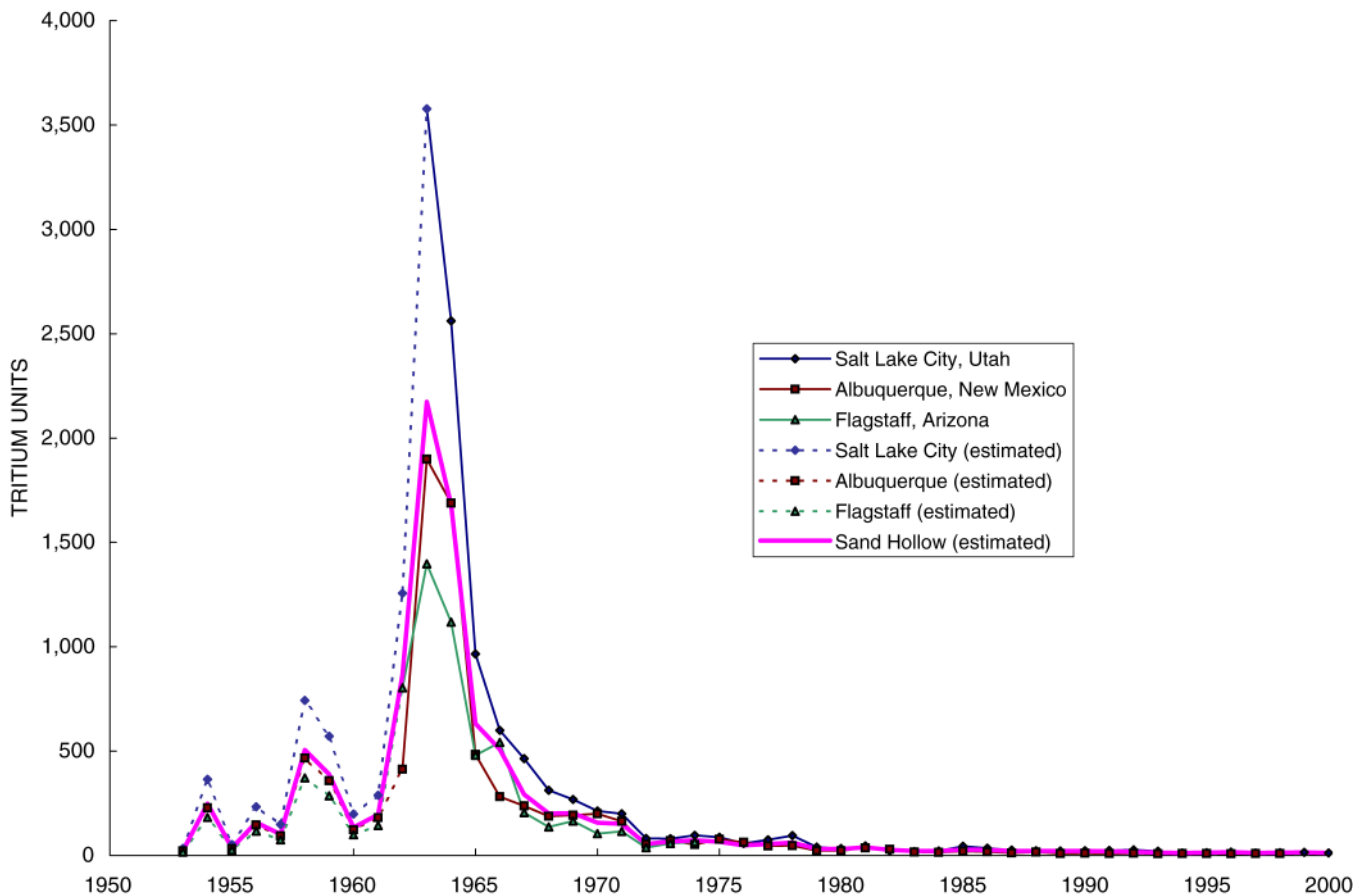


Fig. 5. Estimated tritium concentration of precipitation at Sand Hollow, UT, 1953 to 2000.

25 mm yr⁻¹ because of the potential for higher runoff than at Site 43. Unfortunately, this could not be confirmed because of inaccessibility to drilling. Lower TDTP net-infiltration rates (2.6 ± 1.2 to 10 ± 2 mm yr⁻¹) were measured at Sites 37, 39, and 50, which are covered by loamy sands or loams. The other four sites without discernible ³H peaks are also covered with loamy fine sand or loam.

Net-infiltration rates and uncertainties were also calculated at 11 borehole sites by using the TMB method, with rates ranging from 1.2 ± 0.6 to 14.7 ± 6 mm yr⁻¹ using Eq. [5] and [A7] (Table 4). The mass of vadose zone tritium, M_{VZ} , ranged from 1.5 ± 0.3 tritium-unit meters (TU-m) at Site 38 to 17 ± 2 TU-m at Site 44. Uncertainty in the mass of vadose zone tritium was based on the average precision of the ³H concentration (ranging from 0.2 to 0.5 TU) and water content (ranging from 0.003 to 0.008) for each borehole site. The decay-corrected mass of tritium in precipitation at Sand Hollow, M_{PPT} , is estimated to be 274 ± 54 TU-m for boreholes drilled in 1999 and 246 ± 58 TU-m for boreholes drilled in 2001. Uncertainty in the decay-corrected mass of tritium in precipitation at Sand Hollow was estimated based on the average ratio of atmospheric ³H at Sand Hollow to that at the three closest measurement stations (Salt Lake City/Sand Hollow = 1.29, Albuquerque/Sand Hollow = 0.82, and Flagstaff/Sand Hollow = 0.86).

At the seven sites where both ³H methods were applied, the ratio of the mass-balance to depth-to-peak net-infiltration rates was used as a correction factor for the sites where only the mass-balance method was applied. This correction factor ranged from 1.5 to 2.3; therefore, the reported net-infiltration rates based on borehole ³H in Table 3 for the four sites without TDTP rates (2, 12, 27, 38) are the TMB method rates of Table 4 multiplied by an average correction factor of 2.0. The use of this correction factor assumes that the depth-to-peak method is more accurate than the mass-balance method, which requires an estimate of historical ³H precipitation concentrations. Use of the average annual weighted masses of ³H in precipitation may be the cause of this underestimation of actual net infiltration. As determined from groundwater stable isotope ratios that are more depleted than the average annual concentrations, most net infiltration and recharge at Sand Hollow occurs in the winter. This is also the season of minimum atmospheric ³H concentrations in the northern hemisphere, which would cause the actual mass of ³H in winter recharge to be less than predicted using average annual ³H concentrations. This smaller number in the denominator of Eq. [5] would mean higher actual TMB recharge rates, possibly similar to the TDTP rates.

Groundwater ³H concentrations within Sand Hollow ranged from below detection (0.01) to almost 7

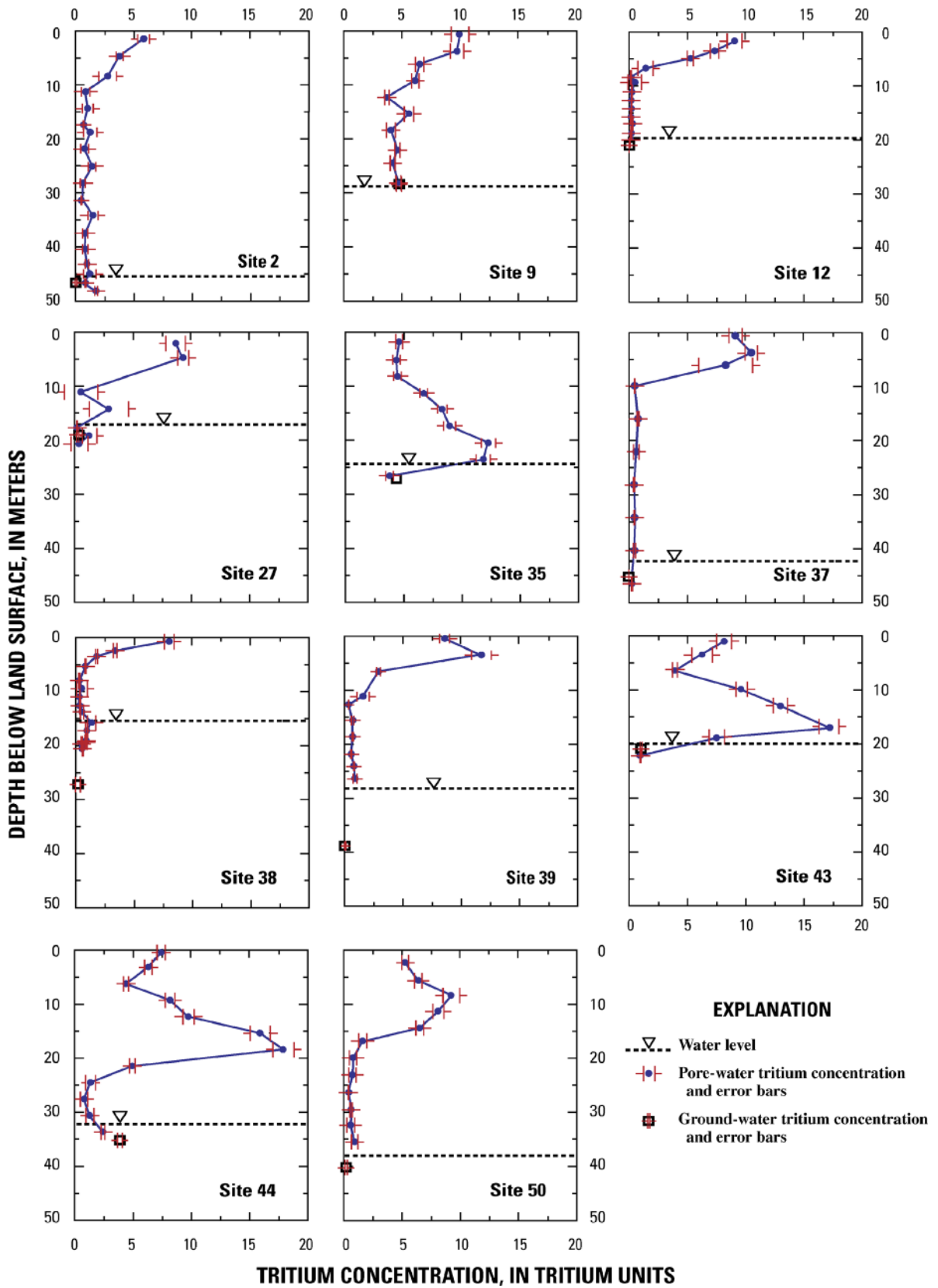


Fig. 6. Tritium concentration of pore-water and groundwater samples collected from selected boreholes in Sand Hollow, UT.

Table 4. Vadose zone tritium parameters and water content from borehole-core samples, Sand Hollow, UT. Refer to Fig. 2 for site numbers.

Site†	Borehole	Collection date	Depth to ³ H peak in vadose zone m	Mean vadose zone volumetric water content to ³ H peak %	Time since peak atmospheric tritium concentration yr	High-recharge sites Low-recharge sites	Depth-to-peak recharge rate‡ mm yr ⁻¹	Mass of tritium in vadose zone TU-m	Mass balance recharge rate§ mm yr ⁻¹	Correction factor for ³ H mass balance recharge rate
9	WD 6	14 May 2001	¶ > 28.7	7.9	38	High-recharge sites	¶ > 57 ± 7	12.9 ± 1.4	¶ > 11 ± 5	-
35	Hole N	25 May 2001	20.3	4.9	38	High-recharge sites	26 ± 3	15.3 ± 1.6	13.1 ± 6	2.0
44	WD 8	17 May 2001	18.6	7.0	38	High-recharge sites	34 ± 5	17.2 ± 2.2	14.7 ± 6	2.3
43	Hole O	10 June 2001	17.4	5.9	38	High-recharge sites	27 ± 4	13.6 ± 1.4	11.6 ± 5	2.3
50	WD 7	15 May 2001	8.4	4.7	38	High-recharge sites	10 ± 2	6.9 ± 1.0	5.9 ± 3	1.8
37	WD 9	22 May 2001	3.8	4.6	38	Low-recharge sites	4.6 ± 2.1	3.5 ± 0.4	3 ± 1.3	1.5
38	Basin 1	22 Apr. 1999	-	-	-	Low-recharge sites	-	1.5 ± 0.3	1.2 ± 0.6	-
12	IFP 1	19 Apr. 1999	-	-	-	Low-recharge sites	-	1.9 ± 0.3	1.4 ± 0.6	-
39	Slope 1a	26 Apr. 1999	3.5	2.7	36	Low-recharge sites	2.6 ± 1.2	2.2 ± 0.4	1.7 ± 0.8	1.6
27	Wash 1	15 Apr. 1999	-	-	-	Low-recharge sites	-	2.7 ± 0.4	2.0 ± 0.9	-
2	Slope 2	3 May 1999	-	-	-	Low-recharge sites	-	2.8 ± 0.8	2.1 ± 1.1	-

† Vadose zone tritium not analyzed from borehole core samples at Sites 4 and 46.

‡ Based on Eq. [3].

§ Based on Eq. [5]; the decay-corrected mass of tritium in precipitation since 1950 is 274 tritium-unit meters for wells drilled in 1999 and 246 tritium-unit meters for wells drilled in 2001.

¶ Based on assumption that tritium peak is already below water table at 28.7 m.

TU (Table 3). Precipitation falling at Sand Hollow more than 50 yr ago would likely have a present-day ³H concentration of <0.5 TU because of radioactive decay. Groundwater ³H concentrations >0.5 TU indicate that precipitation during the past 50 yr has reached the water table. Wells containing water with ³H concentrations >0.5 TU at Sand Hollow are screened within 4 m of the water table (Heilweil, 2003). There is an inverse correlation ($r^2 = 0.77, n = 45$) between Cl⁻ concentrations and ³H concentrations in groundwater at Sand Hollow (Fig. 7), indicating that high-recharge areas correspond to sites where infiltrating precipitation undergoes less evaporative solute concentration in the root zone.

Stable Isotopes

Deuterium (δ²H) ratios of 35 precipitation samples collected during 1999 through 2002 at Sand Hollow ranged from +4.2 to -126.4‰; oxygen-18 (δ¹⁸O) ratios range from +3.3 to -15.5‰. These samples were used to construct the local meteoric water line (LMWL; Fig. 8):

$$\delta H = 7.61\delta^{18}O - 0.03 \quad [6]$$

The slope and y-intercept of the LMWL are similar to published precipitation-isotope data from other arid locations in the southwestern United States (Welch and Preissler, 1986), but the slope and intercept are less than the global meteoric water line (Craig, 1961).

Stable-isotope ratios in vadose zone pore waters range from -47 to -113‰ for δ²H and from +0.5 to -14.0‰ for δ¹⁸O and show most variability in the shallower part of the vadose zone, converging to the groundwater value at or near the water table (Fig. 9). This indicates that little pore-water mixing occurs in the vadose zone compared with that within the aquifer. Pore-water samples from high-recharge sites (Sites 9, 43, 44, 50) have a mean δ²H concentration of -88‰, whereas pore waters from low-recharge sites (Sites 2, 4, 12, 27, 37, 38, 39, 46) have a mean δ²H ratio of -75‰ and follow an evaporative trend below the LMWL (Fig. 8). The slope of this evaporative trend is 3.1, similar to the calculated slope of about 4 for arid settings with low relative humidity (Gat, 1971). The evaporative shift for each pore-water sample was quantified by calculating the expected δ¹⁸O ratio with the measured δ²H ratio and the LMWL given in Eq. [6]. The evaporative shift calculated for each site is the average value from land surface to the water table (Table 3). The smallest shift of 2.1‰ at the highest recharge site (Site 9) and the largest shift of 4.7‰ at the lowest recharge site (Site 4) supports the hypothesis that less evaporative loss occurs where infiltrating water moves quickly beneath the root zone in the more active recharge areas of the basin.

Groundwater stable isotopic ratios at 34 sites in Sand Hollow range from -79 to -94‰ for δ²H (mean of -86‰) and -9.7 to -11.9‰ for δ¹⁸O (mean of -11.3‰). These ratios have a much narrower range than precipitation and vadose zone pore waters and plot closer to the local meteoric water line, showing less evaporative effects than the vadose zone pore waters (Fig. 8). The groundwater stable isotope ratios at each site compare closely with water from vadose zone core samples at or near the

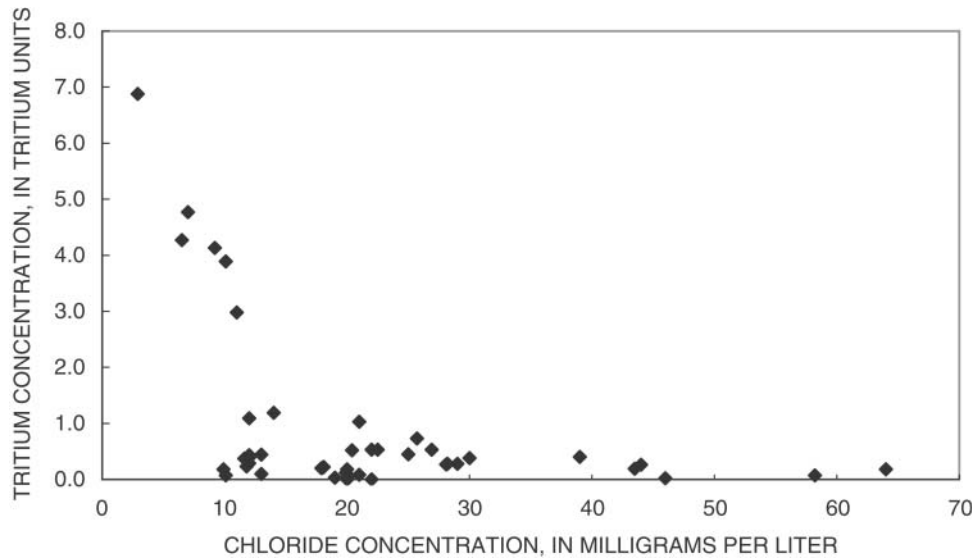


Fig. 7. Relation of tritium concentration to chloride concentration in water from selected wells in Sand Hollow, UT.

water table, confirming that minimal isotopic fractionation occurred during the cryodistillation process. The similarity between stable isotopes in groundwater and in pore waters that contain low Cl^- and high ^3H concentrations shows that these high-recharge sites are where most aquifer recharge occurs.

DISCUSSION

Several environmental tracer techniques were used to evaluate vadose zone processes, compare net-infiltration and recharge rates, and examine spatial and temporal variability. This approach provides a higher level of confidence

than that obtained from any one method by itself and allows for comparison of net infiltration and recharge at different time scales. At Sand Hollow, vadose zone ^3H targets modern (post-1950s) net infiltration whereas vadose zone Cl^- provides a longer-term record of net infiltration (as long as about 12 000 yr at Sand Hollow). Groundwater Cl^- provides more spatially averaged recharge estimates than vadose zone methods because of horizontal hydraulic gradients and mixing in the well screen. Stable isotopes ($\delta^2\text{H}$ and $\delta^{18}\text{O}$), although not providing recharge rates, are useful for evaluating both spatial and temporal differences in net infiltration and recharge.

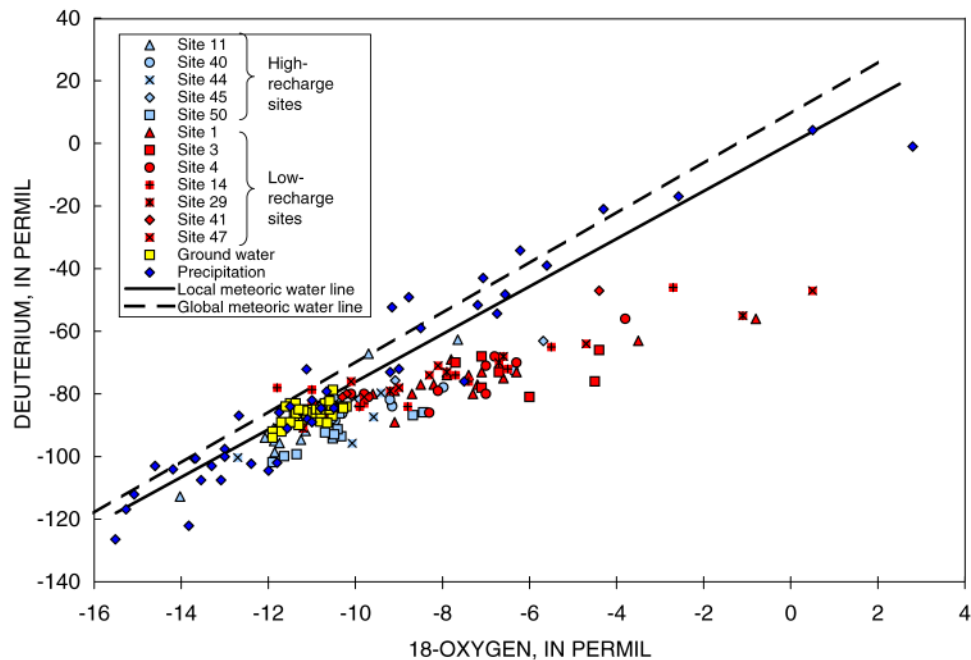


Fig. 8. Relation between stable-isotope ratios of deuterium and oxygen in vadose zone pore water, water samples from selected wells, and precipitation in Sand Hollow, UT.

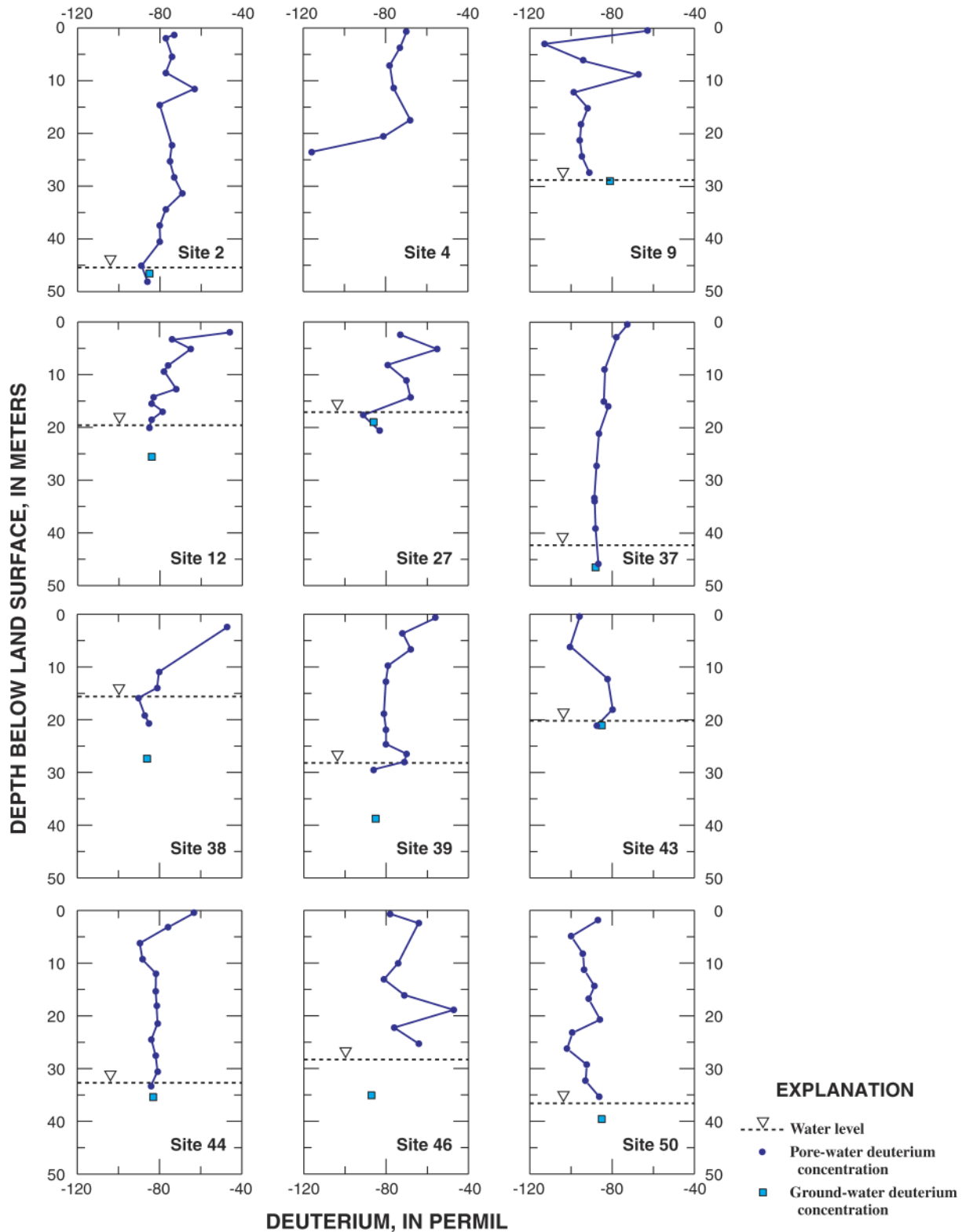


Fig. 9. Stable isotope ratio of deuterium in pore-water and groundwater samples collected from selected wells in Sand Hollow, UT.

Smooth vadose zone Cl^- and ^3H bulges characteristic of those occurring in unconsolidated desert soils were observed in many of the boreholes, an unusual finding for fractured bedrock and indicative of the predominance of matrix-dominated vadose zone flow in the

Navajo Sandstone. This is contrary to an earlier study of shallow vadose zone trenches at Sand Hollow, which found lower solute accumulations in high-angle fractures than in the adjacent matrix at depths between 3 and 6 m below the bedrock surface (Heilweil and Solomon, 2004).

This indicates that preferential flow associated with fractures may be most prominent in the shallowest part of the vadose zone, possibly caused by ponding at the bedrock contact during and after large precipitation events and channeling through near-surface caliche-coated fractures. This water may subsequently be imbibed into more-permeable adjacent sandstone at greater depths where fracture coatings were observed to decrease, explaining the apparent matrix-dominated environmental tracer distributions observed in boreholes. This is supported by a recent numerical modeling study of net infiltration in the Navajo Sandstone (Ludwig, 2003) that demonstrated that unlined fractures with 1-mm apertures (typical of those observed in trenches at Sand Hollow) do not readily saturate and therefore do not act as flow conduits. Rather, water is quickly imbibed by the highly porous sandstone.

Spatial Variability

Net-infiltration and recharge rates at the various sites in Sand Hollow vary greatly, with most recharge occurring in areas that receive focused run-on or have exposed bedrock (sites 9, 43, 44; Fig. 2). Interestingly, substantial amounts of direct net infiltration and recharge also occur beneath coarser-grained sandy soils away from washes (sites 35, 50). This is contrary to findings generally reported from alluvial desert basins receiving similar amounts of precipitation, where little or no basin-floor recharge away from washes occurs under present climatic conditions (Phillips, 1994; Prudic, 1994; Tyler et al., 1996; Andraski, 1997; Izbicki et al., 2002). The results of this study indicate that a higher percentage of water is able to pass beyond the maximum rooting depth and become net infiltration where permeable bedrock formations are exposed or shallowly buried by coarse-grained soils. Low net-infiltration and recharge rates are measured at sites with fine-grained soils receiving little surface-water runoff (sites 2, 4, 12, 27, 37, 38, 39, 46). These loamy soils have a larger water storage capacity, making more infiltrating water available for recycling back to the atmosphere via evaporation and transpiration. Large variations in net-infiltration rates at other study sites in the desert southwestern U.S. receiving similar amounts of precipitation have also been attributed to soil coarseness (Scanlon et al., 2003).

The tracers used in this study generally show similar trends in spatial variability, even though net-infiltration and recharge rates at individual sites vary depending on the particular environmental-tracer method. For example, sites having higher Cl^- and ^3H -based net-infiltration and recharge estimates generally display smaller amounts of vadose zone Cl^- accumulation, higher shallow groundwater ^3H concentrations, smaller vadose zone $\delta^{18}\text{O}$ shifts, and less depleted $\delta^2\text{H}$ values than sites with lower estimated rates (Table 3). Net-infiltration rates calculated from ^3H concentrations are well correlated with rates determined with Cl^- from both within and below the Cl^- bulge ($r^2 = 0.83$ and 0.67 , respectively). Net-infiltration and recharge rates calculated using the three different Cl^- mass-balance methods at each site (within the bulge, below the bulge, below the water table) are also generally

well correlated. However, at Sites 39 and 46, pore-water Cl^- concentrations decrease substantially when crossing from the deep vadose zone into the underlying water table, resulting in much higher groundwater Cl^- -based rates ($15 \pm 7 \text{ mm yr}^{-1}$) than those based on vadose zone Cl^- within the bulge (0.1 ± 0.05 and $0.05 \pm 0.02 \text{ mm yr}^{-1}$, respectively) and vadose zone Cl^- beneath the bulge (3 ± 1 and $4 \pm 1 \text{ mm yr}^{-1}$, respectively). This may be caused by higher-elevation areas with higher recharge rates and a large horizontal component of groundwater flow.

Although they cannot provide direct estimates of recharge rates, groundwater stable isotope ratios and groundwater ^3H concentrations can be used for evaluating spatial variability of recharge. Using the average $\delta^2\text{H}$ values of -75‰ for the low-recharge site vadose zone pore waters, -88‰ for the high-recharge site vadose zone pore waters, and -86‰ for groundwater, a two-end-member mixing model indicates that about 85% of groundwater recharge in Sand Hollow occurs at high-recharge sites. The spatial distribution of groundwater ^3H data indicates that this recharge is concentrated primarily in the part of the basin covered by coarser soils or exposed bedrock (Tables 1 and 3, Fig. 2). Only 5 of 45 groundwater sites within Sand Hollow had values of 0.6 TU or more, an indicator of recent recharge arriving at the water table.

Site-Specific Temporal Variability

Temporal variation in the spatial distribution of net infiltration at Sand Hollow occurs and is likely caused by processes such as climate change (variability in precipitation, temperature, vegetation), caliche formation, erosion, the migration of eolian sand dunes, and changing ephemeral wash locations. The latter has likely occurred at Sites 27 and 38. Unlike the other 11 boreholes, these sites are located in or near the main ephemeral wash of Sand Hollow and do not fit the trend of increasing peak concentration of the shallow Cl^- bulge with increasing total vadose zone Cl^- accumulation (Table 1). Considering the total accumulation of Cl^- in the vadose zone at Site 27 ($72 \pm 8 \text{ mg } 100 \text{ mm}^{-2}$), the peak Cl^- concentration is less than expected. Although this site is situated in the main ephemeral wash, solute distributions in nearby trench excavations indicate that the wash had recently migrated from a location farther to the east (Heilweil and Solomon, 2004). The lower-than-expected peak concentration of the shallow Cl^- bulge at this site is consistent with a recent shift to higher net infiltration beneath the active wash channel, which would push downward and dilute a preexisting shallow Cl^- bulge. The high total cumulative vadose zone Cl^- at the site indicates that the previously accumulated Cl^- has not yet been flushed out of the vadose zone.

The opposite trend may have occurred at Site 38. The very shallow 2-m depth of the Cl^- peak and the higher-than-expected $14\,700 \text{ mg L}^{-1}$ peak concentration at this site (Table 1) indicates a recent change to lower net-infiltration rates and increased run-on of Cl^- . This site is located adjacent to a section of the ephemeral wash that was impounded by a small levee built by cattle ranchers about 50 yr ago (L. Jessup, Washington

County Water Conservancy District, personal communication, 2001) and is now covered with about 0.5 m of fine-grained silts that have settled out of surface-water runoff. Before the existence of the levee, the site was likely a higher recharge site on the natural wash channel. This would explain the low Cl^- concentrations measured below a 3-m depth, the poor correlation between total Cl^- accumulation and peak Cl^- concentration, the low vadose zone ^3H -based net-infiltration rate, and a small average vadose zone $\delta^{18}\text{O}$ evaporative shift (2.2‰) similar to the highest recharge sites (Table 3). The very high Cl^- concentration in the shallow subsurface likely represents a combination of salt accumulation from run-on and evaporative enrichment associated with decreased infiltration through the shallow, low-permeability silts at the site.

Basin-Scale Temporal Variability

Net infiltration at Sand Hollow is episodic and dominated by large but infrequent precipitation events. Moving 30-d precipitation totals for St. George show that two-thirds (10 of 15) of the 30-d periods during the 20th century with more than 100 mm of precipitation occurred during 1957 to 1997. The larger amounts of precipitation during the latter part of the 20th century may have flushed down Cl^- that previously accumulated in the shallow soils. This vadose zone Cl^- accumulation in Sand Hollow is driven by evaporatranspiration within the root zone, consisting primarily of soils above the bedrock contact. This would account for the average 5-m depth for vadose zone Cl^- peaks, much greater than the maximum root zone depth of about 1.5 m at the soil–bedrock interface (Table 1). Periodic flushing, or alternating wetter and drier periods, may also explain double peaks in the Cl^- bulges at Sites 2, 4, and 39 in Fig. 3 (and also at Sites 9, 27, 44, and 50, which are not discernible in the figure). Such downward flushing of Cl^- has been both observed (Stonestrom et al., 2003; Scanlon et al., 2005) and modeled (Scanlon et al., 2003) in the Armagosa Desert of southwestern Nevada.

For the group of 11 sites with vadose zone ^3H information, the ^3H -based net-infiltration rates are much higher ($2.4 \pm 1.2 \text{ mm yr}^{-1}$ to more than $57 \pm 7 \text{ mm yr}^{-1}$; geometric mean of 9 mm yr^{-1} ; Table 3) than rates calculated by using shallow vadose zone Cl^- within the bulge (0.08 ± 0.04 to $8 \pm 4 \text{ mm yr}^{-1}$; geometric mean of 0.4 mm yr^{-1}). At the high-recharge sites, the tritium peak is generally present at greater depths than the bottom of the Cl^- bulge, indicating that the bulge CMB rates should be representative of modern (post-1950s) net infiltration. However, the much-lower CMB rates, compared with ^3H -based rates, indicate that differing processes affect the two tracers. Possibilities include (i) downward vapor transport of ^3H , (ii) run-on of additional Cl^- at each site, or (iii) relict Cl^- from a previously dry period before the latter half of the 20th century not completely flushed downward or diluted by recently higher net infiltration. Thermally induced vapor transport of tritiated water has been previously invoked to explain observed deeper bomb-pulse ^3H (1963) peaks versus ^{36}Cl (1954) peaks in the vadose zone at sites in

New Mexico and Texas (Phillips et al., 1988; Scanlon, 1992). However, the ^3H -based net-infiltration rates at the high-recharge sites in Sand Hollow are a factor of about seven times higher than the Cl^- bulge CMB rates, which is difficult to explain by vapor transport, especially because the generally high water contents (5.4–7.8% Table 1) indicate the predominance of liquid-phase flow. Alternatively, additional Cl^- input associated with run-on could potentially increase Cl^- concentrations and decrease apparent CMB recharge rates. However, the ratio of ^3H versus Cl^- -bulge net-infiltration rates of 4 to 8 at Sites 9 and 44 beneath intermittent washes are similar to ratios ranging from 3 to 13 at Sites 35, 43, and 50 in interdrainage areas away from washes with no expected run-on. Sites having substantial amounts of additional Cl^- input from run-on would presumably have much higher ratios than sites not receiving run-on. Therefore, the explanation of relict Cl^- from previous centuries under drier conditions remains as the most likely hypothesis for the lower CMB rates, although some vapor-phase ^3H transport is also possible. This is supported by calculated Cl^- accumulation inventories within the bulges ranging from 50 to 400 yr, representing older net infiltration than the ^3H peaks (Table 1).

The $^3\text{H}/\text{Cl}^-$ bulge net-infiltration rate ratios at the low-recharge sites are much higher (7–80, mean = 40) than the high-recharge site ratios (3 to 13, mean = 7). At these low-recharge sites, the bottom of the Cl^- bulge is much deeper than the bomb-pulse tritium, so this Cl^- clearly represents conditions before the latter half of the 20th century. The Cl^- accumulation within these bulges ranges from about 800 to 7000 yr (Table 1). Even if the CMB rates at the low net-infiltration sites are adjusted upward using an average $^3\text{H}/\text{Cl}^-$ bulge net-infiltration ratio of 7 for the high-recharge sites, the ^3H -based rates are still, on average, about sixfold higher. This indicates that net-infiltration rates during the mid- to late-Holocene were much lower than in recent decades.

Comparison of ^3H -based net-infiltration rates to deeper vadose zone CMB net-infiltration rates beneath the Cl^- bulge is not as straightforward. For the group of high-recharge sites (9, 35, 43, 44, 50), vadose zone ^3H -based net-infiltration rates ($10 \pm 2 \text{ mm yr}^{-1}$ to more than $57 \pm 7 \text{ mm yr}^{-1}$) are higher than vadose zone Cl^- -based rates from beneath the bulge (3 ± 2 to $13 \pm 7 \text{ mm yr}^{-1}$), also indicating higher rates in recent decades than during previous centuries. For the group of low-recharge sites (2, 12, 27, 37, 38, 39), however, vadose zone ^3H -based net-infiltration rates (2.4 ± 1.2 to $4.6 \pm 2.1 \text{ mm yr}^{-1}$) are similar to vadose zone Cl^- -based rates beneath the bulge (2 ± 1 to $5 \pm 2 \text{ mm yr}^{-1}$). This deeper Cl^- represents the oldest preserved vadose zone information on net infiltration at Sand Hollow and indicates that rates earlier in the Holocene were similar to the higher rates of recent decades. Unlike the high-recharge sites, the total amount of Cl^- beneath the bulge at these low-recharge sites is a small fraction of the total vadose zone Cl^- accumulation (3–33%), consistent with higher rates earlier in the Holocene.

Four of the 12 borehole sites drilled to the water table have shallow groundwater ^3H concentrations of more

than 0.5 TU, indicating some recent recharge. The CMB recharge rates based on groundwater chloride at these sites range from 9 ± 4 to 60 ± 29 mm yr⁻¹, very similar to the vadose zone ³H-based net-infiltration rates of 10 ± 2 to $>57 \pm 7$ mm yr⁻¹. This close agreement between water-table and vadose zone tracers in areas with short vadose zone residence times indicates an equilibration between net infiltration, vadose zone movement, and groundwater recharge. This contrasts recent studies showing long-term drying conditions and upward water transport in alluvial interbasin areas with deep water tables in response to the Pleistocene–Holocene climate shift (Walvoord et al., 2002a; Scanlon et al., 2003).

Eight of the 12 borehole sites drilled to the water table have shallow groundwater ³H concentrations <0.5 TU, indicating recharge that occurred more than 50 yr ago. Recharge rates based on groundwater Cl⁻ concentrations at these eight boreholes range from 3 ± 1.4 to 15 ± 7 mm yr⁻¹, higher than the 0.5 ± 0.2 to 5 ± 2 mm yr⁻¹ based on vadose zone Cl⁻ beneath the bulge (Table 3). As discussed, higher groundwater Cl⁻-based recharge rates may be caused by higher recharge in up-gradient higher-elevation areas. However, another possibility is that the groundwater Cl⁻-based recharge rates indicate a wetter climatic period earlier in the Holocene.

The dominance of winter (cool season) net infiltration and recharge at Sand Hollow is evident by the uniformity of groundwater stable isotope ratios at the more negative end of the range of precipitation values. Currently, about 55% of precipitation in Sand Hollow occurs during November through March and 35% during August through October. Spring is extremely dry, accounting for only 10% of the annual precipitation (Western Regional Climate Center, 2004). However, groundwater at sites receiving recent recharge, as indicated by ³H concentrations >1 TU, has less depleted $\delta^2\text{H}$ values (-79 to -84‰) than the $\delta^2\text{H}$ values (-84 to -88‰) of older groundwater (<0.5 TU; Table 3). Previous carbon-14 analyses indicate that all of the groundwater in Sand Hollow is of Holocene age (Heilweil, 2003), discounting the possibility that the older, more isotopically depleted groundwater had been recharged during the cooler late Pleistocene climate. Rather, the isotopic enrichment of recent recharge may indicate increased summer monsoonal precipitation during the wetter latter part of the 20th century. This is consistent with recent findings suggesting that the 1950s drought coincided with decreased summer monsoonal precipitation (Gray et al., 2003). Southwestern Utah is located in the transitional area between winter Pacific-storm dominated precipitation to the north and west and a bimodal combination of winter Pacific storms and summer Gulf of California and Gulf of Mexico monsoon precipitation to the east and south (Brenner, 1974; Weng and Jackson, 1999). Therefore, the occurrence of summer monsoonal precipitation and recharge at Sand Hollow may be very sensitive to slight changes in atmospheric circulation patterns. Another possibility is the strengthening El Niño during recent decades (Trenberth and Hoar, 1997; McPhaden, 1999), which may bring warmer southern Pacific (versus cooler northern Pacific) winter precipitation to the region.

The environmental tracer data at Sand Hollow indicate that a full swing in climatic cycle has occurred, with higher net-infiltration and recharge rates earlier in the Holocene changing to lower rates in the later Holocene, returning again to higher rates during recent decades. Recent higher net infiltration and recharge is consistent with both St. George, UT, and regional precipitation records. Greater-than-average precipitation occurred in the Colorado Plateau and Rocky Mountain region from 1977 through 1998, possibly linked with the positive warm phase of the Pacific Decadal Oscillation (PDO) and a cool phase of the Atlantic Multidecadal Oscillation (AMO) (Gray et al., 2003). With regards to the longer-term record, tree-ring based precipitation reconstructions spanning the period of 1226 through 2001 in the nearby Uintah Basin show that the last four decades of the 20th Century make up the second-wettest multidecadal period of the past 775 yr (Gray et al., 2004). These tree-ring paleo-reconstructions also show an extremely dry period from about 1430 to 1786 CE, during which there were nine multi-decadal droughts yet only four multidecadal wet periods. This and other late-Holocene dry periods may have caused the large accumulation of Cl⁻ in the shallow vadose zone bulges at Sand Hollow. The higher net-infiltration rates earlier in the Holocene calculated from deeper vadose zone Cl⁻ beneath the bulge are consistent with lake-sediment core data (pollen and plant microfossil records) from the nearby Kolob Plateau of northern Arizona, indicating very wet conditions during the early Holocene and late Pleistocene (Weng and Jackson, 1999). Similar Holocene variations in recharge to the Navajo Sandstone are inferred from groundwater flow modeling and Cl⁻, ³⁶Cl, and ¹⁴C data at Black Mesa, AZ (Zhu, 2000; Zhu et al., 2003), which showed recharge varying from as little as 4% of precipitation during the late Holocene to as much as about 8% of precipitation during the late Pleistocene and early Holocene.

Comparison with Alluvial Desert Vadose Zones

Studies by Walvoord et al. (2002a, 2002b) and Scanlon et al. (2003) showed that in alluvial interdrainage areas in the arid southwestern United States, transport is generally dominated by upward water movement due to drying conditions during the Holocene, resulting in zero or negative net infiltration. Scanlon et al. (2003) showed that at some sites this upward movement is vapor, whereas at other sites it is liquid water. Shallow vadose zone matric potential measurements at these sites in Texas and Nevada are typically as negative as about -1000 m water. Measured matric potentials at Sand Hollow are generally less negative than these desert alluvial sites. Nested heat-dissipation probes installed for a 2.5-yr period at Site 39 show matric potentials ranging from about -15 to -0.2 m water at depths from 5 to 30 m, with little seasonal variation (Fig. 10). Because of the uniform hydraulic properties of the Navajo Sandstone and similar relatively high water contents at this and the other low-recharge sites (about 2–8%), the matric potentials at Site 39 are likely representative of most low-recharge areas within Sand Hollow. Higher water contents in-

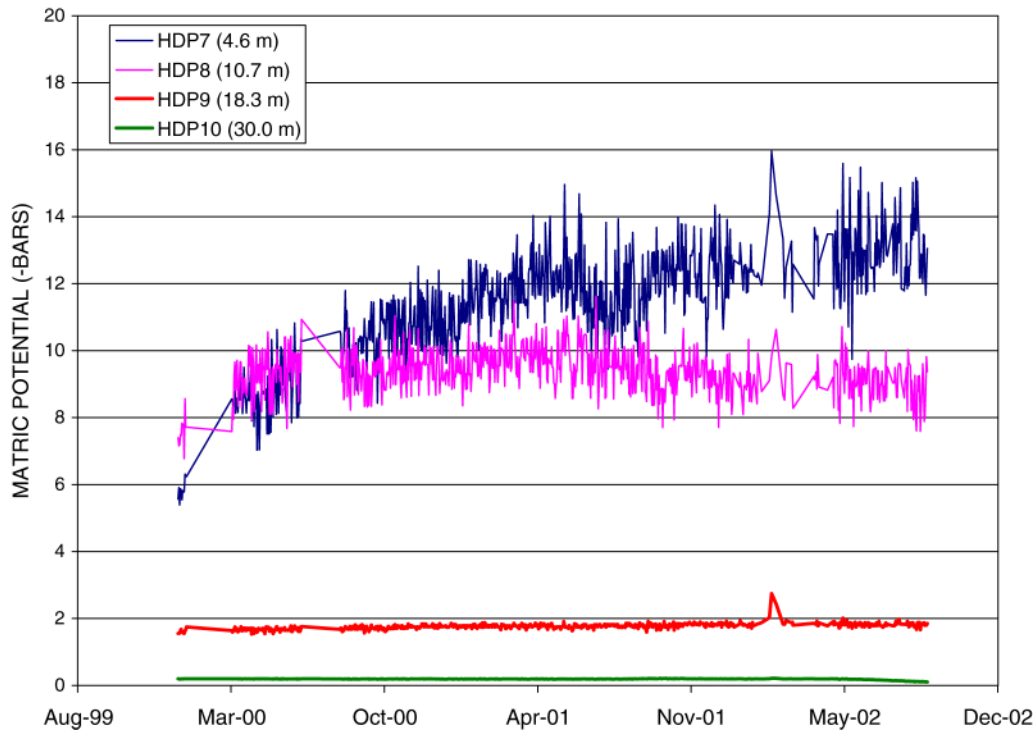


Fig. 10. Vadose zone water potential measured with heat-dissipation probes at various depths below land surface at Site 39, Sand Hollow, UT.

dicates that matric potentials are even less negative at higher-recharge sites. Preliminary data, therefore, indicate that the vadose zone of the Navajo Sandstone at Sand Hollow is much wetter than other desert alluvial basins, and water movement is primarily downward. However, additional research is needed to further investigate whether upward water movement occurs in the driest parts of the basin.

CONCLUSIONS

A combination of vadose zone and groundwater environmental tracers was used to evaluate net infiltration and recharge at Sand Hollow, including site-specific (spatial) processes and seasonal to millennial temporal variations. Profiles of vadose zone Cl^- and ^3H show smooth patterns similar to those observed in desert soils, indicating that net infiltration and recharge through the Navajo Sandstone is matrix dominated rather than fracture controlled. However, net-infiltration and recharge rates are generally higher than in unconsolidated desert soils because the sandstone allows water movement but not root penetration. Spatial variations show that net infiltration and recharge are highest in the 50% of the basin covered by coarser soils and exposed bedrock. Pore-water stable isotope ratios indicate that about 85% of recharge occurs in these high-infiltration areas. Estimates of net-infiltration rates based on vadose zone ^3H range from 2.4 ± 1.2 to more than $57 \pm 7 \text{ mm yr}^{-1}$. Net-infiltration rates based on vadose zone Cl^- range from 0.03 ± 0.01 to $13 \pm 7 \text{ mm yr}^{-1}$. Recharge rates based on groundwater Cl^- range from 3 ± 1.4 to $60 \pm 29 \text{ mm yr}^{-1}$. Sites with higher vadose zone ^3H - and Cl^- -based net-infiltration

rates generally also have lower vadose zone Cl^- accumulations, lower vadose zone evaporative ^{18}O shifts, lower groundwater Cl^- concentrations, and higher groundwater ^3H concentrations. Because of the different time periods represented by these environmental tracers, it is inferred that recharge rates at Sand Hollow have changed from higher rates earlier in the Holocene to lower rates during the past few centuries or millenia, back to higher rates during the latter part of the 20th century.

APPENDIX: UNCERTAINTY ANALYSIS

A method based on Ang and Tang (1975) was used to evaluate uncertainty (variance) in atmospheric Cl^- deposition, net infiltration, and recharge rates at Sand Hollow. For a function Y composed of n statistically independent variables:

$$Y = f(X_1, X_2, \dots, X_n), \quad [\text{A1}]$$

the first order approximation of the mean, \bar{Y} , and variance, $\text{Var}(Y)$ can be defined, respectively, as

$$\bar{Y} \approx f(\bar{X}_1, \bar{X}_2, \dots, \bar{X}_n), \quad [\text{A2}]$$

and

$$\begin{aligned} \text{Var}(Y) = & \left(\frac{\partial Y}{\partial X_1} \right)^2 \text{Var}(X_1) + \left(\frac{\partial Y}{\partial X_2} \right)^2 \text{Var}(X_2) + \dots \\ & + \left(\frac{\partial Y}{\partial X_n} \right)^2 \text{Var}(X_n) \end{aligned} \quad [\text{A3}]$$

where the partial derivatives $(\partial Y / \partial X_n)$ are evaluated at the mean value of the parameter.

Based on Eq. [A2], the uncertainty in the vadose zone and groundwater CMB recharge rate, q_{Cl} , is defined as

$$\text{Var}(q_{Cl}) = \left(\frac{\partial q_{Cl}}{\partial [Cl_{dep}]} \right)^2 \text{Var}[Cl_{dep}] + \left(\frac{\partial q_{Cl}}{\partial [Cl_{pw}]} \right)^2 \text{Var}[Cl_{pw}] + \left(\frac{\partial q_{Cl}}{\partial P} \right)^2 \text{Var}[P] \quad [A4]$$

where Cl_{pw} represents either the vadose zone or groundwater Cl^- concentration. The uncertainty, or variance, in the Cl^- vadose zone residence time, T_R , is defined as

$$\text{Var}(T_R) = \left(\frac{\partial T_R}{\partial M_{Cl}} \right)^2 \text{Var}[M_{Cl}] + \left(\frac{\partial T_R}{\partial [Cl_{dep}]} \right)^2 \text{Var}[Cl_{dep}] + \left(\frac{\partial T_R}{\partial V_P} \right)^2 \text{Var}[V_P] \quad [A5]$$

The uncertainty in the TDTP recharge rate, q_{TDTP} , is defined as

$$\text{Var}(q_{TDTP}) = \left(\frac{\partial q_{TDTP}}{\partial [z]} \right)^2 \text{Var}[z] + \left(\frac{\partial q_{TDTP}}{\partial [\theta_v]} \right)^2 \text{Var}[\theta_v] + \left(\frac{\partial q_{TDTP}}{\partial t} \right)^2 \text{Var}[t] \quad [A6]$$

The uncertainty in the TMB recharge rate, q_{TMB} , is defined as

$$\text{Var}(q_{TMB}) = \left(\frac{\partial q_{TMB}}{\partial M_{Vz}} \right)^2 \text{Var}[M_{Vz}] + \left(\frac{\partial q_{TMB}}{\partial [M_{PPT}]} \right)^2 \text{Var}[M_{PPT}] + \left(\frac{\partial q_{TMB}}{\partial P} \right)^2 \text{Var}[P] \quad [A7]$$

ACKNOWLEDGMENTS

This material is based on work supported by the Washington County Water Conservancy District, the Lower Colorado River Basin Office of the U.S. Bureau of Reclamation, and the Ground-Water Resources Program of the U.S. Geological Survey. The authors gratefully acknowledge the pore-water anion analysis performed by Laura Wolfsberg with the support of June Fabryka-Martin of Los Alamos National Laboratory, the atmospheric deposition anion analysis performed by John Izbicki of the USGS, and the vegetation survey performed by William Pockman of the University of New Mexico. Many of the ideas were developed through conversations with Warren Wood and Alan Flint of the USGS. The authors also thank David Susong and Rick Healy of the USGS for their helpful suggestions on drafts of the report.

REFERENCES

Allison, G.B. 1988. A review of some of the physical, chemical, and isotopic techniques available for estimating groundwater recharge. p. 49–72. *In* I. Simmers (ed.) Estimation of natural groundwater recharge. D. Riedel Publishers, Norwell, MA.

Allison, G.B., G.W. Gee, and S.W. Tyler. 1994. Vadose zone techniques for estimating groundwater recharge in arid and semi-arid regions. *Soil Sci. Soc. Am. J.* 58:6–14.

Allison, G.B., and M.W. Hughes. 1978. The use of environmental

chloride and tritium to estimate total recharge to an unconfined aquifer. *Austr. J. Soil Resour.* 16:181–195.

Andraski, B.J. 1997. Soil-water movement under natural-site and waste-site conditions: A multiple-year field study in the Mojave Desert, Nevada. *Water Resour. Res.* 33:1901–1916.

Ang, A.H.-S., and W.H. Tang. 1975. Probability concepts in engineering planning and design. Vol. 1. Basic principles. John Wiley & Sons, New York.

Brenner, I.S. 1974. A surge of maritime tropical air—Gulf of California to the southwestern United States. *Monthly Weather Rev.* 102:375–389.

Clark, W.B., W.J. Jenkins, and Z. Top. 1976. Determination of tritium by mass spectrometric measurements of ^3He . *Int. J. Appl. Radiat. Isot.* 27:515–522.

Cook, P.G., I.D. Jolly, F.W. Leaney, G.R. Walker, G.L. Allan, L.K. Fifield, and G.G. Allison. 1994. Unsaturated zone tritium and chlorine 36 profiles from southern Australia: Their use as tracers of soil water movement. *Water Resour. Res.* 31:1709–1719.

Cordova, R.M. 1978. Ground-water conditions in the Navajo Sandstone in the central Virgin River basin, Utah. *Tech. Publ. 61. Utah Dep. of Nat. Resour., Salt Lake City, UT.*

Cordova, R.M. 1981. Ground-water conditions in the upper Virgin River and Kanab Creek basins area, Utah, with emphasis on the Navajo Sandstone. *Tech. Publ. 70. Utah Dep. of Nat. Resour., Salt Lake City, UT.*

Cordova, R.M., G.W. Sandberg, and W. McConkie. 1972. Ground-water conditions in the central Virgin River basin, Utah. *Tech. Publ. 40. Utah Dep. of Nat. Resour., Salt Lake City, UT.*

Craig, H. 1961. Isotopic variations on meteoric waters. *Science (Washington, DC)* 133:1702–1703.

Danielson, T.W., and J.W. Hood. 1984. Infiltration to the Navajo Sandstone in the lower Dirty Devil River basin, Utah, with emphasis on techniques used in its determination. *USGS Water-Resour. Invest. Rep.* 84-4154.

Davis, S.N., J.T. Fabryka-Martin, and L.E. Wolfsberg. 2004. Variations of bromide in potable groundwater in the United States. *Groundwater* 42:902–909.

Davis, S.N., D.O. Whitemore, and J. Fabryka-Martin. 1998. Uses of chloride/bromide ratios in studies of potable water. *Groundwater* 36:338–350.

Dettinger, M.D. 1989. Reconnaissance estimates of natural recharge to desert basins in Nevada, U.S.A., by using chloride-balance calculations. *J. Hydrol. (Amsterdam)* 106:55–78.

Eriksson, E. 1983. Stable isotopes and tritium in precipitation. p. 19–33. *In* Guidebook on nuclear techniques in hydrology. IAEA, Vienna.

Eychaner, J.H. 1983. Geohydrology and effects of water use in the Black Mesa area, Navajo and Hopi Indian Reservations, Arizona. *USGS Water-Supply Paper* 2201.

Flint, A.L., L.E. Flint, E.M. Kwicklis, J.T. Fabryka-Martin, and G.S. Bodvarsson. 2002. Estimating recharge at Yucca Mountain, Nevada, USA: Comparison of methods. *Hydrogeol. J.* 10:180–204.

Friedman, I., G.I. Smith, J.D. Gleason, A. Warden, and J.M. Harris. 1992. Stable isotope composition of waters in southeastern California: 1. Modern precipitation. *J. Geophys. Res.* 97(D5):5795–5812.

Gat, J.R. 1971. Comments on the stable isotope method in regional ground-water investigations. *Water Resour. Res.* 7:980–993.

Gray, S.T., J.L. Betancourt, C.L. Fastie, and S.T. Jackson. 2003. Patterns and sources of multidecadal oscillations in drought-sensitive tree-ring records from the central and southern Rocky Mountains. *Geophys. Res. Lett.* 30(6):1316. doi:10.1029/2002GL016154.

Gray, S.T., S.T. Jackson, and J.L. Betancourt. 2004. Tree-ring based reconstructions of interannual to decadal scale precipitation variability for northeastern Utah since 1226 A.D. *J. Am. Water Resour. Assoc.* 40:947–960.

Heilweil, V.M. 2003. Recharge to the Navajo Sandstone aquifer of southwestern Utah. Ph.D. diss. University of Utah, Salt Lake City.

Heilweil, V.M., G.W. Freethey, B.J. Stolp, C.D. Wilkowske, and D.E. Wilberg. 2000. Geohydrology and numerical simulation of groundwater flow in the central Virgin River basin of Iron and Washington Counties, Utah. *Tech. Publ. 116. Utah Dep. of Nat. Resour., Salt Lake City, UT.*

Heilweil, V.M., and D.K. Solomon. 2004. Millimeter- to kilometer-scale variations in vadose zone bedrock solutes: Implications for estimating recharge in arid settings. p. 49–67. *In* J.F. Hogan et al.

- (ed.) Groundwater recharge in a desert environment: The southwestern United States. Water Science and Applications Ser. 9. Am. Geophys. Union, Washington, DC.
- Hood, J.W., and T.W. Danielson. 1981. Bedrock aquifers in the lower Dirty Devil River basin area, Utah, with special emphasis on the Navajo Sandstone. Tech. Publ. 68. Utah Dep. of Nat. Resour., Salt Lake City, UT.
- Hood, J.W., and D.J. Patterson. 1984. Bedrock aquifers in the northern San Rafael Swell area, Utah, with special emphasis on the Navajo Sandstone. Tech. Publ. 78. Utah Dep. of Nat. Resour., Salt Lake City, UT.
- International Atomic Energy Agency Global Network of Isotopes in Precipitation. 2004. Web Site of the Global Network of Isotopes in Precipitation (GNIP) and Isotope Hydrology Information System (ISOHIS). Available at <http://isohis.iaea.org> (accessed 23 May 2005, verified 25 Oct. 2005). Isotope Hydrology Section, IAEA, Vienna, Austria.
- Izbicki, J.A., J. Radyk, and R.L. Michel. 2002. Movement of water through the thick unsaturated zone underlying Oro Grande and Sheep Creek Washes in the western Mojave Desert, USA. *Hydrogeol. J.* 10:409–427.
- Kimball, B.A. 1992. Geochemical indicators used to determine source of saline water in Mesozoic aquifers, Montezuma Canyon area, Utah. p. 89–106. *In* S. Subitzky (ed.) Selected papers in the hydrologic sciences, 1988–1992. USGS Water Supply Paper 2340.
- Ludwig, D.E. 2003. Numerical simulation of tritium transport in an unsaturated fractured sandstone. M.S. thesis. University of Utah, Salt Lake City.
- Maxey, G.B., and T.E. Eakin. 1950. Groundwater in the White River valley, White Pine, Nye and Lincoln Counties, Nevada. Nevada State Engineer, Water Resour. Bull. 8.
- McPhaden, M.J. 1999. Genesis and evolution of the 1997–98 El Niño. *Science* (Washington, DC) 283:950–954.
- Naftz, D.L., Z.E. Peterman, and L.E. Spangler. 1997. Using $\delta^{87}\text{Sr}$ values to identify sources of salinity to a freshwater aquifer, greater Aneth Oil Field, Utah, USA. *Chem. Geol.* 141:195–209.
- National Atmospheric Deposition Program. 1999–2003. National Atmospheric Deposition Program. Available at <http://nadp.sws.uiuc.edu/> (accessed 1 Apr. 2005, verified 25 Oct. 2005). NADP, Illinois State Water Survey, Champaign, IL.
- Nimmo, J.R., D.A. Stonestrom, and K.C. Akstin. 1994. The feasibility of recharge rate determinations using the steady-state centrifuge method. *Soil Sci. Soc. Am. J.* 58:49–56.
- Phillips, F.M. 1994. Environmental tracers for water movement in desert soils of the American Southwest. *Soil Sci. Soc. Am. J.* 58:15–24.
- Phillips, F.M., J.L. Mattick, and T.A. Duval. 1988. Chlorine 36 and tritium from nuclear weapons fallout as tracers for long-term liquid movement in desert soils. *Water Resour. Res.* 24:1877–1891.
- Prudic, D.E. 1994. Estimates of percolation rates and ages of water in unsaturated sediments at two Mojave Desert sites, California–Nevada. USGS Water-Resour. Invest. Rep. 94-4160.
- Rasmussen, T.C., and D.D. Evans. 1993. Water infiltration into exposed fractured rock surfaces. *Soil Sci. Soc. Am. J.* 57:324–329.
- Robson, S.G., and E.R. Banta. 1995. Groundwater atlas of the United States. Segment 2: Arizona, Colorado, New Mexico, Utah. USGS Hydrologic Invest. Atlas 730-C.
- Scanlon, B.R. 1992. Evaluation of liquid and vapor flow in desert soils based on chlorine-36 and tritium tracers and nonisothermal flow simulations. *Water Resour. Res.* 28:285–297.
- Scanlon, B.R. 2000. Uncertainties in estimating water fluxes and residence times using environmental tracers in an arid unsaturated zone. *Water Resour. Res.* 36:395–409.
- Scanlon, B.R., R.W. Healy, and P.G. Cook. 2002. Choosing appropriate techniques for quantifying groundwater recharge. *Hydrogeol. J.* 10: 18–39.
- Scanlon, B.R., K. Keese, R.C. Reedy, J. Simunek, and B.J. Andraski. 2003. Variations in flow and transport in thick desert vadose zones in response to paleoclimatic forcing (0–90 kyr): Field measurements, modeling, and uncertainties. *Water Resour. Res.* 39(7):1179. doi:10.1029/2002WR001604.
- Scanlon, B.R., R.C. Reedy, D.A. Stonestrom, D.E. Prudic, and K.F. Dennehy. 2005. Impact of land use and land cover change on groundwater recharge and quality in the Southwestern U.S. *Global Change Biol.* 11:1577–1593.
- Stonestrom, D.A., D.E. Prudic, R.J. Lacznak, K.C. Akstin, R.A. Boyd, and K.K. Henkelman. 2003. Estimates of deep percolation beneath Irrigated fields, native vegetation, and the Amargosa River channel. Amargosa Desert, Nye County, Nevada. USGS Open-File Rep. 03-104.
- Trenberth, K.E., and T.J. Hoar. 1997. El Niño and climate change. *Geophys. Res. Lett.* 24:3057–3060.
- Tyler, S.W., J.B. Chapman, S.H. Conrad, D.P. Hammermeister, D.O. Blout, J.J. Miller, M.J. Sully, and J.M. Ginnani. 1996. Soil-water flux in the southern Great Basin, United States: Temporal and spatial variations over the last 120,000 years. *Water Resour. Res.* 32:1481–1499.
- Walvoord, M.A., Phillips, F.M., Tyler, S.W., and Hartsough, P.C., 2002b. Deep arid system hydrodynamics. 2: Application to paleo-hydrologic reconstruction using vadose zone profiles from the northern Mohave Desert. *Water Resour. Res.* 38(12):1291. doi: 10.1029/2001WR000825.
- Walvoord, M.A., M.A. Plummer, G.M. Phillips, and A.V. Wolfsberg. 2002a. Deep arid system hydrodynamics. 1. Equilibrium states and response times in thick desert vadose zones. *Water Resour. Res.* 38(12):1308. doi:10.1029/2001WR000824.
- Welch, A.H., and A.M. Preissler. 1986. Aqueous geochemistry of the Bradys Hot Springs geothermal area, Churchill County, Nevada. p. 17–36. *In* S. Subitzky (ed.) Selected Papers in the Hydrologic Sciences. USGS Water-Supply Paper 2290.
- Weng, C., and S.T. Jackson. 1999. Late Glacial and Holocene vegetation history and paleoclimate of the Kaibab Plateau, Arizona. *Paleogeogr. Paleoclimatol. Paleocol.* 153:179–201.
- Western Regional Climate Center. 2004. Western Regional Climate Center. Historical Climate Information. Monthly and annual precipitation at St. George, Utah (Station 427516). Available at <http://www.wrcc.dri.edu> (accessed 11 Feb. 2004, verified 25 Oct. 2005). WRCC, Reno, NV.
- Wood, W.W., and W.E. Sanford. 1995. Chemical and isotopic methods for quantifying ground-water recharge in a regional, semi-arid environment. *Groundwater* 33:458–468.
- Zhu, C. 2000. Estimate of recharge from radiocarbon dating of groundwater and numerical flow and transport modeling. *Resour. Res.* 36:2607–2620.
- Zhu, C., J.R. Winterle, and E.I. Love. 2003. Late Pleistocene and Holocene groundwater recharge from the chloride mass balance method and chlorine-36 data. *Water Resour. Res.* 39(7):1182. doi: 10.1029/2003WR001987.